Resonance of Cable-Stayed Bridges Subjected to Delayed Time-Histories Using Multi-Support Excitation

Bashar Hariri

A Thesis

in

The Department

of

Building, Civil and Environmental Engineering

Presented in Partial Fulfillment of the Requirements

for the Degree of Master of Applied Science (Civil Engineering) at

Concordia University

Montreal, Quebec, Canada

December 2018

CONCORDIA UNIVERSITY

School of Graduate Studies

This is to certify that the thesis prepared

By: Bashar Hariri

Entitled: Resonance of Cable-Stayed Bridges Subjected to Delayed Time-Histories Using Multi-Support Excitation

and submitted in partial fulfillment of the requirements for the degree of

Master of Applied Science (Civil Engineering)

complies with the regulations of the University and meets the accepted standards with respect to originality and quality.

Signed by the final examining committee:

Dr. A. M. Hanna Chair, Examiner

Dr. R. Ganesan Examiner

Dr. M. Nik-Bakht Examiner

Dr. L. Lin Supervisor

Approved by _____

Chair of Department or Graduate Program Director

December 2018 _____

Dean of Faculty

ABSTRACT

Resonance of Cable-Stayed Bridges Subjected to Delayed Time-Histories Using Multi-Support Excitation

Bashar Hariri

The requirement for the seismic analysis of cable-stayed bridges under spatially varying loads is not well defined in the bridge design codes around the world. The Canadian Highway Bridge Design Code briefly stipulates that it is the responsibility of the designer to check the effect of the spatially varying loads while no details are provided. Given this, the objective of this study is to evaluate the seismic performance of cable-stayed bridges using multi-support excitation. For the purpose of the study, Quincy Bayview Bridge located in Illinois, USA is selected for the analysis. Ten ground motion acceleration time-histories obtained from earthquakes in the US, Japan, and Taiwan are used as initial seismic excitation to be applied on the bridge. They are then converted to displacement time-histories and applied at each support by considering the phase delay of the wave traveling from one support to another. The seismic analysis using multi-support excitation shows that significant vertical deck displacement is produced, which is generally ignored in the analysis of cable-stayed bridges under uniform excitation. The response curve for the vertical deck displacement *vs* wave velocity demonstrates that a resonance-like condition is triggered at relatively low velocity. A mathematical formula is developed to account for the potential of resonance for the displacement of the deck in the vertical direction. Furthermore, a time delay factor of 0.72 is proposed to estimate the critical seismic wave velocity that would trigger the resonance. In addition, the results from this study indicate that attention is required for

the bridge response in the direction orthogonal (e.g., vertical direction) to the direction of the seismic loading (e.g., horizontal direction), while multi-support excitation should be considered for this purpose.

ACKNOWLEDGMENT

I would like to express my great appreciation to my supervisor Dr. Lan Lin for her guidance and support, which has introduced me to the academic and scientific research world. I also wish to acknowledge the financial support provided by the Natural Sciences and Engineering Research Council (NSERC), the Aide Financière Aux Études (AFE), and Concordia University Faculty of ENCS graduate scholarship through the course of this study.

My sincere thanks are due to my parents whom their prayers surrounded me and will always be there for me. Most importantly, I would like to thank my wife, Rama for believing in me and for her endless support during my years of study at Concordia.

TABLE OF CONTENTS

LIST OF FIGURES

LIST OF TABLES

Chapter 1

INTRODUCTION

1.1 Background

The origin of cable-stayed bridges can be dated back as early as late 15th century when a Venetian inventor Fausto Veranzio provided a sketch of the first bridge of this kind. With the improvement of our knowledge on structure design, construction and computer science, cable-stayed bridges have drawn significant attention of the engineering community around the world. According to the recent statistics data, among the fifty longest cable-stayed bridges, forty-two of them were built in the 20th century; another twenty bridges will be open to the public between 2018 and 2019. Furthermore, the maximum span length of cable-stayed bridges has increased significantly. For example, it was about 500 m at the late 1990s, however, it recently has been doubled to reach around 1.1km (Russky Bridge, Russia, completed in 2012).

Cable-stayed bridges are very unique due to their extremely long span length, high pylons/towers, complicated connections between elements, and anchoring systems. It is well known that cable-stayed bridges are very sensitive to vibration due to wind and/or earthquake loads. Given this, dynamic analysis is always preferred to examine their performance.

For the design and evaluation of cable-stayed bridges for earthquake loads, it is more appropriate to conduct time-history analysis considering the importance category and the complexity of the bridge. For seismic analysis of short-span bridges, all the supports can be assumed to be excited simultaneously, i.e., they are under uniform seismic excitation. However, this assumption would not be valid for cable-stayed bridges due to its extremely long span length. Therefore, spatial effects including wave passage effect, incoherence effect, and foundation effect, which are ignored in the analysis of short-span bridges, may not be ignored in the seismic analysis of cable-stayed bridges. The causes of each of the above-mentioned effects are as follows,

- Wave passage effect or phase effect is due to the fact that seismic waves arrive at different pier supports at different times (Kiuregihan and Neuenhofer 1992),
- Incoherence effect is due to reflection and refraction in heterogeneous soil medium, which makes the ground motion lose its coherency. It further leads to the superposition of waves arriving from extended sources (Kiuregihan and Neuenhofer 1992),
- Foundation effect is due to the fact that foundation and soil may not vibrate at the same phase and the same amplitude given their different flexibility (Sextos et al. 2003). For example, a pier foundation might be stiffer than the surrounding soil or vice versa.

It is generally reported that non-uniform excitation (also referred to as multi-support excitation) is appropriate for time-history analysis of cable-stayed bridges under

earthquake loads, i.e., different excitations are assigned at different supports. Among the three effects discussed above, only the wave passage effect was considered in this study as the other two are soil-specific matters.

1.2 Objective of the study

The objective of this study is to examine the displacement of cable-stayed bridges in vertical direction under phase-delayed seismic time-histories. In addition, a methodology for determination of a critical velocity of seismic waves that triggers resonance-like condition of bridge in vertical direction is provided. To achieve these objectives, the following steps are followed

a) Create a finite element model of an existing cable-stayed bridge using SAP2000

b) Verify the dynamic properties of the model

c) Select a set of earthquake records for time-history analysis

d) Assign non-uniform excitation to bridge supports and conduct time-history analysis for each record for different seismic wave velocities

e) Evaluate the potential of resonance in bridge vertical direction, and

f) Validate findings on generic typical cable-stayed bridges

1.3 Outline of the thesis

This thesis is organized into five chapters and two appendixes including this chapter. Chapter 2 serves as literature review; Chapter 3 provides a description of the bridge in question along with the development of a finite element model of the bridge while detailed research work is presented in Chapter 4 and the main conclusions from the study are given in Chapter 5.

Chapter 2 summarizes previous studies on the seismic analysis of cable-stayed bridges under non-uniform excitation. The response parameters and the critical loading direction to assign the excitation considered by researchers in the past are also discussed in this chapter. In addition, the requirements for the seismic analysis of cable-stayed bridges stipulated in the current American, Canadian and European bridge design codes are highlighted.

Chapter 3 describes Quincy Bayview Bridge considered in this study along with the finite element model developed for the structural analysis. Validation of the model is also discussed in this chapter.

Chapter 4 focuses on investigation of the bridge seismic response under multi-support excitation. A potential of bridge resonance in the vertical direction under the loading in the longitudinal direction is the core of discussion. A formula and a factor for a time delay for resonance are proposed.

Chapter 5 summarizes the main findings and conclusions from this study.

Chapter 2

LITERATURE REVIEW

2.1 Past studies on spatial effects on seismic loads

Spatially varying load method is necessary for time-history analysis of cable-stayed bridges, in which different excitations are assigned to different supports. This is mainly because the amplitude and/or the phase of seismic waves will decay when they travel from one support to another given the span length of a cable-stayed bridge is relatively long in some cases reaching a kilometre. Therefore, the normal practice of considering the uniform excitation for time-history analysis of short- and medium-span bridges is not valid anymore.

Researchers have established two approaches to consider the non-uniformity of a seismic wave when it travels from one support to another within a span. For ease of discussion, they are referred to as Approach I and Approach II hereafter. Approach I focuses on the nature of wave travelling with time to include the decay of its amplitude and/or the its phase delay. Approach II ignores the change of the wave when it travels, and focuses on determining the structural response using the theory of dynamic analysis. In simple words, the first method is to consider the spatially varying loading from seismology point of view while the second method is from structure point of view.

2.1.1 Review of studies on Approach I

As described above, the purpose of considering spatial variation of ground motions in seismic analysis is to apply non-uniform excitations at bridge supports. This can be done in three ways,

Method I: Assign different time series at each individual support to consider incoherence effect and/or foundation effect (Kiuregihan and Neuenhofer 1992; Sextos et al. 2003),

Method II: Assign the "same" time series at all supports but a phase delay is considered to derive the excitation at each support. This is to account for the wave passage effect (Kiuregihan and Neuenhofer 1992; Tian and Lou 2014),

Method III: Assign different time series derived with a combination of Methods I and II (Zerva 1991).

Research on considering spatial variation of ground motions started in 1970s when Christian (1976) evaluated five approaches available at that time to estimate the relative movement between two points on the ground during an earthquake event. Since these methods are very simple, the reliability of the results is questionable. Years later, a more advanced method was proposed by O'Rourke et al. (1982), in which the direction of wave propagation was taken into account for the first time. The results from their study show a good agreement between the ground motion arrival times recorded by seismographs during the 1971 San Fernando and 1979 Imperial Valley earthquake and those estimated using the proposed method. However, this method did not account for earthquake source

characteristics, such as, the wave passage effect, or incoherency effect. This is because seismographs were positioned to determine mainly the magnitude of earthquakes and the amplitude of the ground motions.

In 1980, the University of California Berkeley launched **S**trong **M**otion **A**rray in **T**aiwan, **P**hase 1 (SMART-1) project in collaboration with Taiwan Institute of Earth Sciences. The objective of the project was to provide earthquake data for a wide range of research topics and hazard-reduction activities. In total, thirty-seven stations in Taiwan were positioned radially with respect to a station at the center as illustrated in Fig. 2.1. One of the reasons for such array was to help researchers examine the semismic wave propagation during its travelling. The project has collected data from 60 earthquakes with different magnitudes, focal depths, and epicentral distances until 1991.

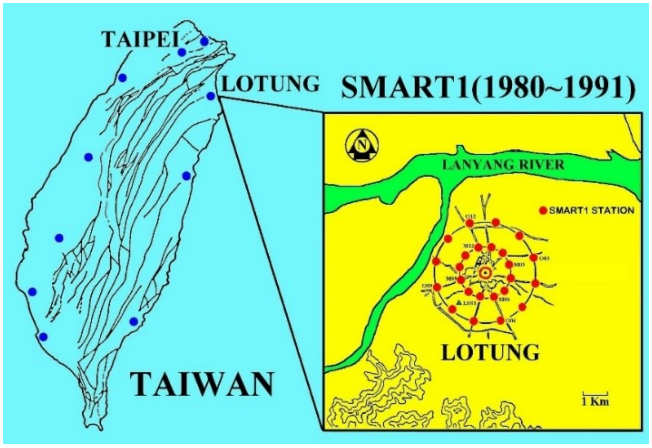

Figure 2.1 Strong motion stations in Taiwan (Online source).

Based on SMART-1 array data, Harichandran and Vanmarcke (1986) investigated wave propagation considering both incoherence and phase effects. They concluded that wave propagation mainly occurred on bedrock. They also reported that the phase effect

became dominant when the seismic waves traveled vertically through soil medium. Loh and Yeh (1988) developed a model to simulate the shear wave propagation. Their findings were consistent with those made in Harichandran and Vanmarcke (1986). Furthermore, they reported that the spatial load variation was dominated by the phase effect.

It is necessary to mention that the above-mentioned studies were focused on examining the characteristics of seismic waves, which is a subject of seismology. However, structural engineers are more interested in the effects of waves on structure responses when they are travelling in the soil. For example, Zerva (1991) carried out a study to investigate the effects of coherence and/or phase of ground motions on continuous beam structures with different spans and different lengths subjected to vertical loading. Zerva (1991) reported that the response of beams based on incoherent ground motions with different phases at supports are identical to the case when the phase is the same at all the supports. In addition, Zerva (1991) concluded that coherency had more effects than phase.

Since considering spatial loading in the seismic analysis is quite complicated, some researchers have attempted to develop a simple method. For example, Li and Li (2004) proposed a response spectrum method to determine structural responses under non-uniform loading based on the framework developed by Heredia-Zavoni and Vanmarcke (1994). The method was then tested on a 2-span continuous bridge, and it was found that the bridge responses were compatible with those using Monte-Carlo simulation. The observation of this study is very encouraging, however, the methodology has not been widely applied. One of the main reasons is because, it requires knowledge of signal processing and heavy mathematical calculations. Aswathy et al. (2013) conducted a study to assess pounding

effects on bridges due to multi-support excitation. It concluded that the phase effect produced larger pounding forces in the piers.

In most of the studies on evaluation of performance of cable-stayed bridges under seismic loads, the input excitations are assigned in the longitudinal direction, and the response parameters examined are those related to design, such as, moments and shears in members, lateral displacement of polygons/towers (Crewe and Norman 2006; Aswathy, et al. 2013; Gong, et al. 2015). The vertical response, e.g., deck displacement, is normally ignored. However, a study performed by Allam and Datta (2003) demonstrated that the excitation in the longitudinal direction activated the response in the vertical direction. This conclusion was confirmed in shake table tests carried out by Yang et al. (2012), which was one of few tests on cable-stayed bridges. The generic bridge considered had three spans (160m+430m+160m) but scaled down to 1:120 for testing. One of the findings from the study was, the wave propagation led to a maximum variation of +50% to -25% compared to the uniform excitation for the vertical displacement of the girder.

The study conducted by Tian and Lou (2014) was intended to examine the relationship between the seismic response and the seismic wave velocity. It reported that non-uniform excitation affected some response parameters, such as, longitudinal displacement of the pier, moment and shear force in the pier. Their study also suggested that resonance would occur due to non-uniform excitation, which in turn would maximize the bridge response.

2.1.2 Reviews of studies on Approach II

Unlike Approach I, Approach II concerns more about the maximum structure response to be considered in the bridge design not the wave itself. According to Chopra (2011) and Jangid (2013), the structure response due to multi-support excitation can be decomposed into two parts, i.e., dynamic response and quasi-static response. The latter is a differential response generated due to different excitations at different supports. Because the quasi-static response depends mainly on structural stiffness, theoretically a "simplified" method can be developed to determine such response. For example, Berrah and Kausel (1993) proposed a so-called modified response spectrum method. Generally speaking, the response spectrum for each support can be developed by using cross-correlation factors with respect to the modal properties. Heredia-Zavoni and Vanmarcke (1994) developed a method for calculating the dynamic response when non-uniform excitation is considered. The concept of spectral moments was introduced as part of the methodology. However, these two methods have not been adopted. This is because additional knowledge is required to fully understand the definition of cross-correlation factors (Berrah and Kausel 1993) and spectral moments (Heredia-Zavoni and Vanmarcke 1994).

2.2 Current codes and guidelines on multi-support excitation

All the guidelines and codes in North America do not have provisions explicitly for conducting seismic analysis for multi-support excitation including Guidelines for the Design of Cable-Stayed Bridges (ASCE 1992), ATC-32 Improved Seismic Design Criteria for California Bridges: Provisional Recommendations (ATC 1996), AASHTO Guide

Specifications for LRFD Seismic Bridge Design (2015), and Canadian Highway Bridge Design Code (2014). Japanese Design Specifications Highway Bridges (2012) also does not provide such guidelines considering Japanese researchers and engenderers are very advanced in earthquake engineering and have tremendous experience in design of cable-stayed bridges.

The Eurocode 8 (2005) is the first code that introduced a detailed method for seismic analysis of bridges under multi-support excitation. The concept of this method is very similar to Approach II discussed obove. According to EC8, variation of the spatial loading shall be considered if, (i) bridge length exceeds (L_g/1.5), or (ii) bridge is constructed on two or more different soil types. The parameter L_g is determined using Table 2.1 depending on soil profile. The definition of soil type is provided in Table 2.2.

Table 2.1 EC8 value of L_g.

EC8 soil profile	A	B	C	D	E
L_g (m)	600	500	400	300	500

Table 2.2 Soil classification (Eurocode 8 2004).

Ground type	Description of stratigraphic profile	Parameters		
		v_s (m/s)	N_{spt}	C_u (kPa)
A	Rock or other rock-like geological formation, including at most 5 m of weaker material at the surface.	>800	-	-
B	Deposits of very dense sand, gravel, or very stiff clay, at least several tens of metres in thickness, characterised by a gradual increase of mechanical properties with depth.	360-800	>50	>250
C	Deep deposits of dense or medium-dense sand, gravel or stiff clay with thickness from several tens to many hundreds of metres.	180-360	15-50	70-250
D	Deposits of loose-to-medium cohesionless soil (with or without some soft cohesive layers), or of predominantly soft-to-firm cohesive soil	<180	<15	<70
E	A soil profile consisting of a surface alluvium layer with v_s values of type C or D and thickness varying between about 5 m and 20 m, underlain by stiffer material with v_s > 800 m/s.			

The step-by-step procedure for EC 8 simplified method is given as follows,

Step 1: Determine relative displacements for two critical modes

The two critical modes are designated as Mode I and Mode II, respectively. In Mode I (Fig. 2.2) the displacements at all the supports have a positive sign while in Mode II the displacement shifts between the positive and the negative sign from one support to another. The relative displacement at support *i* for Mode I and Mode II can be calculated using Equation 2.1 and 2.2, respectively.

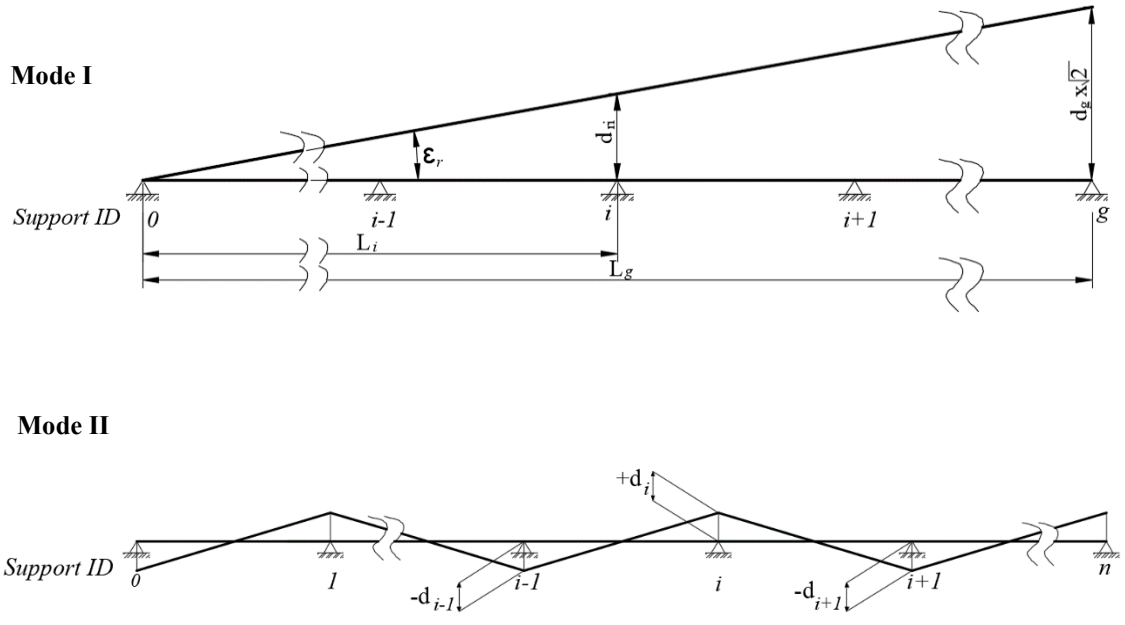

Figure 2.2 Deformed shapes defined in Eurocode 8 (2005).

$$d_{ri} = \varepsilon_r L_i \leq \sqrt{2}\, d_g \tag{2.1}$$

$$d_i = \pm \frac{\Delta d_i}{2} = \frac{\beta_r\, \varepsilon_r\, L_{av,i}}{2} \tag{2.2}$$

In Equation 2.1,

L_i: is the distance of support "i" from a reference support i = 0, that may conveniently be selected at one of the end supports,

ε_r: can be calculated by $\sqrt{2}d_g/L_g$ while L_g is the total length of the bridge,

d_g: is the maximum ground displacement that can be determined by $0.025 \cdot a_g \cdot S \cdot T_c \cdot T_d$,

where a_g is the design ground acceleration; S is soil factor;

T_c is the limit of the constant spectral acceleration branch; and

T_d is the value defining the beginning of the constant displacement response

range of the spectrum.

In Equation 2.2,

β_r: can be taken as 0.5 when all three supports *i-1*, *i*, and *i+1* have the same ground type (same soil). Otherwise, it is taken as 1.0,

$L_{av,i}$: is an average of the distances between the two adjacent spans of the support under consideration $L_{i-1,i}$ and $L_{i+1,i}$

Step 2: Assign the above-calculated displacement at each support for Mode I and Mode II, run static analysis

Step 3: Run dynamic analysis under uniform excitation

Step 4: Combine the responses obtained from Step 2 and Step 3 using SRSS rule

After EC8 simplified method was released, researchers have been working on different types of bridges in order to verify the proposed method (Sextos and Kappos 2005; Crewe and Norman 2006). Below are some of the concerns addressed by these authors,

- The mode shape of the two critical modes specified in EC8 is independent on the characteristics of the input ground motions, such as, frequency content and the amplitude. Accordingly, the response results will depend on the records selected for the dynamic analysis.
- The EC8 simplified approach neglects the dynamic effects of spatial loads and the contribution of higher modes as only two modes are used in the calculation.

- The EC8 simplified method might not be appropriate for bridges with a significant curvature in plan.

2.3 Nonlinearity of cable-stayed bridges

Base on the literature, the nonlinearity of cable-stayed bridges is mainly observed in the bridge geometry, cables, and the flexure behaviour of members (Nazmy and Abdel-Ghaffar 1990). This could be due to either service loads or seismic loads. Unlike short-span bridges, cable-stayed bridges normally demonstrate nonlinear response under self-weight while the materials and members remain elastic. This unique behavior is usually caused by the sag of cables associated with their axial force and deformation relation as reported in Fleming (1978). In addition. the nonlinear flexure behaviour of members is quite often observed in pylons. Therefore, larger axial force in a pylon and/or excessive lateral displacement of the pylon generated by earthquake load will make the ignorance of the P-delta effect impossible in seismic analysis. Furthermore, the nonlinearity of member geometry becomes obvious when deformation is significant. In this case, the bridge stiffness must be modified based on the new geometrical location of the joints (Nazmy and Abdel-Ghaffar 1990).

The nonlinearity of the cables during service loads is represented by an equivalent modified modulus of elasticity of cable (Equation 2.3). The equation was first proposed by Ernst (1965), and is widely accepted by researchers (e.g., Kudder 1968; Leonhardt and Zellner 1980)

$$E_{mod} = \frac{E_{ori}}{1 + \frac{(WL)^2 (EA)_{ori}}{12\, T_0^3}} \tag{2.3}$$

Where,

E_{ori}: is the original cable modulus of elasticity,

EA: is an axial stiffness of the cable,

W: is the weight per unit length of the cable,

L: is the horizontal projected length of the cable,

T_0: is the tension force in the cable.

With respect to the nonlinearity of cable-stayed bridges under seismic loading, Nazmy and Abdel-Ghaffar (1990) proposed a method to account for the nonlinearity for dynamic analysis. Their approach is to determine bridge stiffness considering the nonlinearity of the bridge under normal service loads, and then this stiffness is applied to conduct linear dynamic analysis. Fleming et al. (1983) compared the responses of cable-stayed bridges from three analysis cases, namely, Case I: linear static analysis-linear dynamic analysis, Case II: nonlinear static analysis-linear dynamic analysis, and Case III: nonlinear static analysis-nonlinear dynamic analysis. The above designation of either linear static analysis or nonlinear static analysis refers to the method of determining the bridge stiffness explained in Fleming et al. (1983). They concluded that the results from Case II and III were compatible. They also reported the results from Case I were also acceptable unless the bridge stiffness was determined based on the method proposed in Nazmy and Abdel-Ghaffar (1990) as discussed above.

2.4 Motivation of this study

Most of the studies described above focused on structure responses in the longitudinal direction, which is the direction for the seismic excitation is applied. Few researchers investigated response of cable-stayed bridges in vertical direction. Allam and Datta (2003) reported that seismic excitation in the longitudinal direction affected the responses in the vertical direction, but no detailed discussion was provided. Yang et al. (2012) noticed that vibration in the vertical occurred in some cases due to wave propagation during their shaking table tests. Tian and Lou (2014) proposed a method to consider the effects of time delay between the two pylons in a three-span cable-stayed bridge. The response spectrum method given in Berrah and Kausel (1993) sounds simple, but it requires significant efforts to obtain the correlation factors to proceed with the calculation. On the other hand, EC8 method has significantly simplified the seismic analysis for multi-support excitation. The major drawback of this method is that the dynamic portion of the total response due to non-uniform excitation is replaced by uniform loading.

Given this, the purpose of this study is to understand bridge behaviour in vertical direction by applying different excitations at different supports while all the excitations are assigned in the bridge longitudinal direction. It should be made clear herein that both incoherence and foundation effects are not considered in this study, i.e., only wave effect is considered.

Chapter 3

DESCRIPTION AND MODELLING OF THE BRIDGE

3.1 Description of bridge

Quincy Bayview Bridge (Fig. 3.1) located in Illinois, USA, was selected for this study. This is because, (i) the information on the bridge geometry is well documented as given in Wilson and Gravelle (1991), and (ii) ambient vibration tests' results are available in Wilson and Liu (1991), which is useful for validation of the finite element model developed in the present study. It also should be noted that Quincy Bayview Bridge has been used in several studies as a typical bridge to assess the performance of cable-stayed bridges, e.g., Hua and Wang (1996), Zadeh (2012), Poddar and Rahman (2015), etc.

Figure 3.1 Quincy Bayview Bridge (Photo courtesy: John A.).

As illustrated in Fig. 3.2, the bridge has three spans of 134.2 m + 274.5 m + 134.2 m with a total length of 542.9 m. It is necessary to mention herein that the imperial units used in the original bridge geometrical configuration are converted to metric units in this study. Each side span is supported by 14 cables while the main span is supported by 28 cables. Figure 3.3 presents the configuration of the bridge superstructure. The 230 mm thick deck is made of precast post-tensioned concrete with a total width of 14.17 m. The deck is supported by five steel stringers (W18x119) equally positioned at a center-to-center spacing of 2.21 m, and two main girders at the outer edges of the deck with an overall depth of 1.93 m.

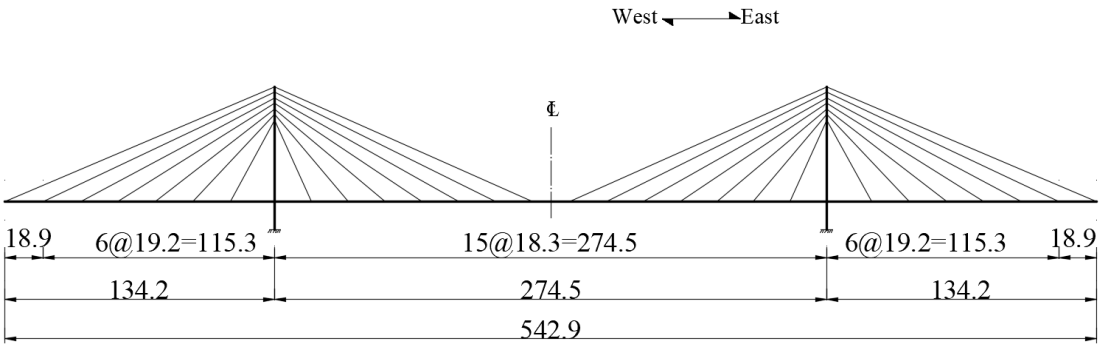

Figure 3.2 Elevation view of the bridge (units: m).

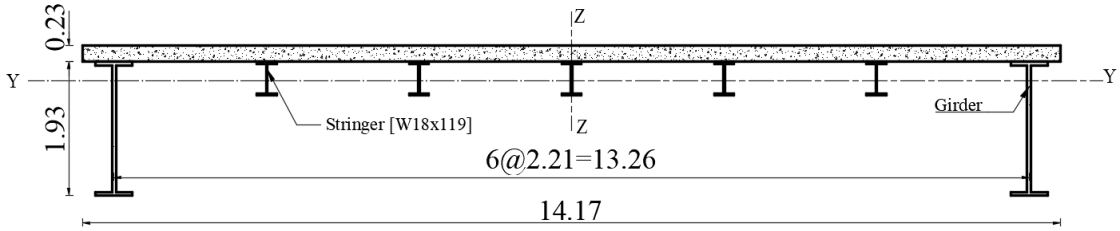

Figure 3.3 Configuration of bridge superstructure (units: m).

The bridge tower consists of H-shaped legs, a lower strut and an upper strut as illustrated in Fig. 3.4. Each leg of the tower has three typical rectangular sections, i.e., Section 1-1, Section 2-2, and Section 3-3, over its height. More specifically, Section 1-1 runs from the base of the leg to the deck level, Section 2-2 extends for 4.7 m above the deck level, and Section 3-3 to the height of the rest of the leg. The lower strut supports the entire superstructure while the upper strut connects the two legs at about 48.8 m measured from the bottom of the leg. There is a 1.2 m thick concrete wall below the lower strut between the two legs to stiffening the tower.

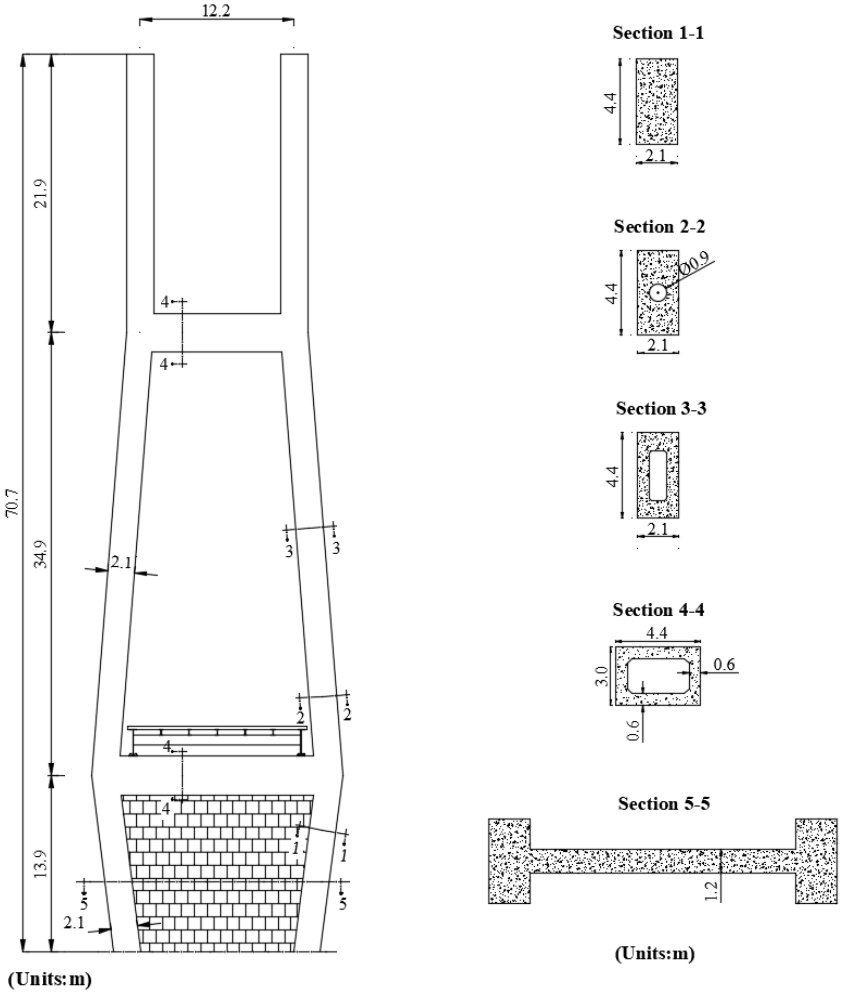

Figure 3.4 Geometry of the bridge pylon.

The superstructure is connected to the towers through two sets of vertical and horizontal bearings at each tower. As shown in Fig. 3.5, there is a vertical bearing under each girder at both towers, which allows the superstructure to slide in the horizontal direction. In addition, there are longitudinal (at the west tower only) and transverse bearings at the towers (Fig. 3.6), in which the longitudinal bearings are fixed to avoid the excessive sliding of the deck and transverse bearings restrain the transverse motions at both towers.

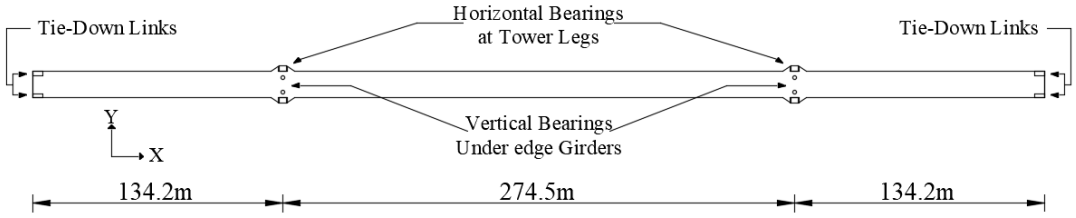

Figure 3.5 Bearing system adopted from Wilson and Gravelle (1991).

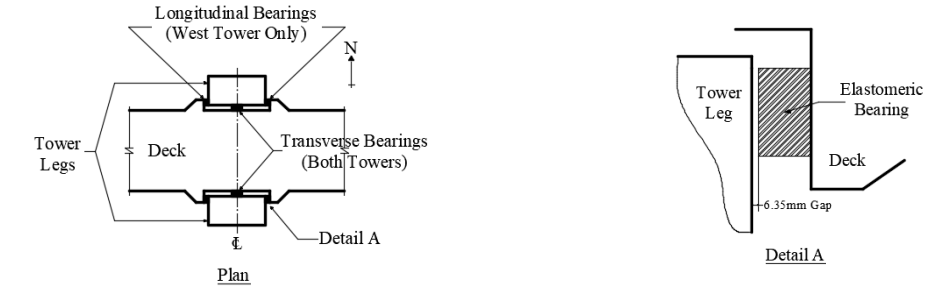

Figure 3.6 Layout of horizontal bearings adopted from Wilson and Gravelle (1991).

The connection between the deck and the abutment at each end was made using a tie-down link (Fig. 3.7) as reported in Wilson and Gravelle (1991). The pins at both sides allow the link to have a free rotation about y-axis, which is perpendicular to the plane. The

lower shoe allows rotation around the central vertical axis of the link. However, this link restricts rotation about the x-axis as well as translation about all the three axes x, y, and z.

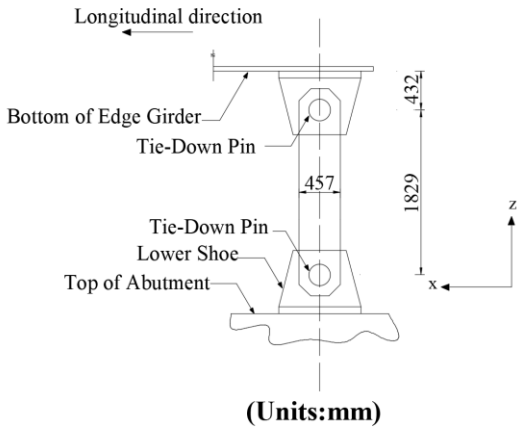

Figure 3.7 Tension-link system adopted from Wilson and Gravelle (1991).

3.2 Modelling of bridge

3.2.1 Deck

In this study, the structural analysis software SAP2000 was used to develop a 3D finite element model (Fig. 3.8). The bridge deck was modeled as a spine with twenty-nine elements in the longitudinal direction, i.e., seven elements in each side span and fifteen elements in the main span where each element connects the anchors between the two adjacent cables.

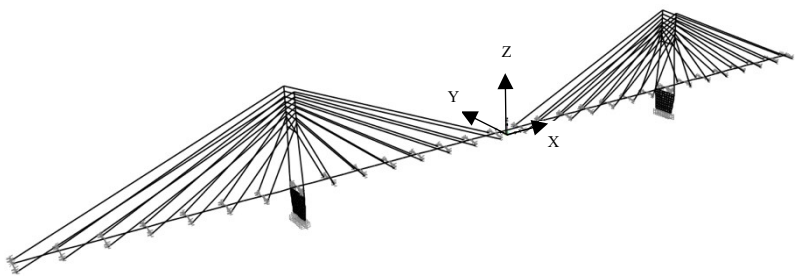

Figure 3.8 Finite element model of the bridge.

In the transverse direction, the bridge superstructure is also modeled as a spine element with a lumped mass on each end through a rigid link in both horizontal and vertical directions as shown in Fig. 3.9a. More specifically, a lumped mass is assigned at 813 mm below the shear center of the composite section on each side, and it is connected by horizontal and vertical massless rigid link elements. The weight of each mass and the length of the vertical links are determined, by considering the lumped mass and the center of gravity of each component in the deck to include the barriers, slab, stringers, and girders as presented in Fig. 3.9b. The length of the horizontal link is measured from center-to-center of cables. Table 3.1 summarizes the translational mass of the superstructure assigned in SAP2000.

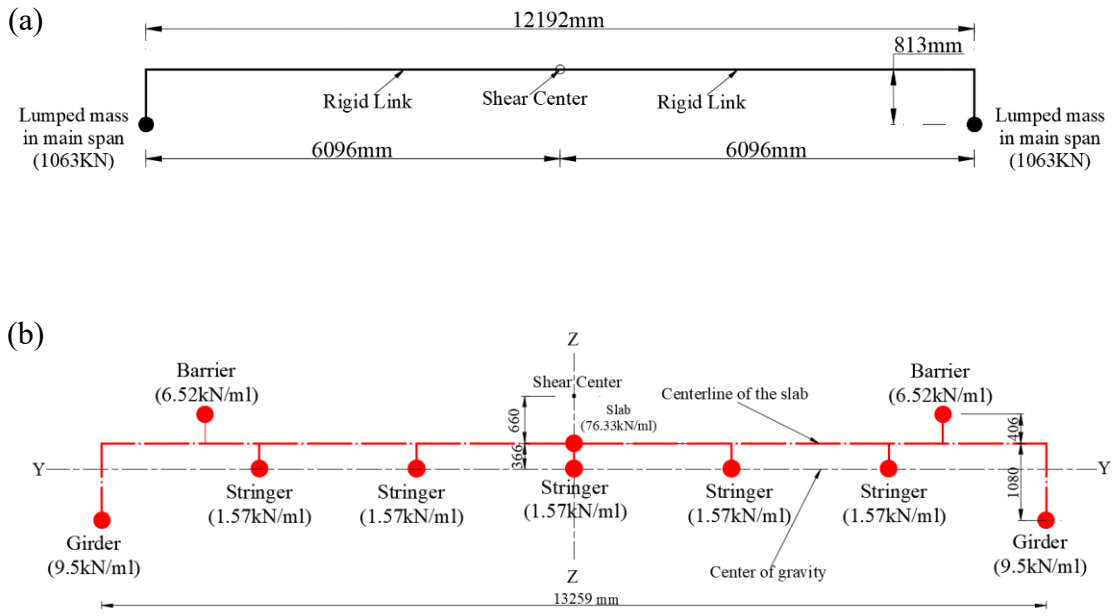

Figure 3.9 Modeling of the superstructure in transverse direction: (a) configuration of the link; (b) distribution of lumped masses.

Table 3.1 Superstructure translational mass assigned in SAP2000.

Element	Weight (kN/m)	Lump weight	
		main span (kN)	side span (kN)
Concrete slab	76.33	1063.0	1115.5
Stringer	1.57		
Girder	9.50		
Barrier	6.52		

The moments of inertia of the superstructure were calculated using built-in function "Section Designer" in SAP2000 while the reference material for the composite section is considered to be steel. It is worth mentioning that the values for the input parameters obtained in this study matched those provided in Wilson and Gravelle (1991) except the moment of inertia around z-z axis (I_{z-z}), where 9% difference was observed. This might be due to the sectional dimensions for built-up girders collected in this study were not as accurate as those when Wilson and Gravelle developed their model. Therefore, a modification factor was applied to I_{z-z} in order to match the value reported in Wilson and Gravelle (1991). In summary, the following values were assigned in SAP2000,

- Moment of inertia around z-z axis = 19.8 m^4, around y-y axis = 0.34 m^4,
- Torsional constant excluding warping = 0.01 m^4,
- Torsional constant including warping = 0.027 m^4.

It is necessary to mention that the rotational mass moments of inertia based on the geometry of the section were modified as suggested by Wilson and Gravelle (1991) to simplify modeling. In order to take into account the effects of wrapping, an equivalent

torsional constant (J_{eq}) provided in Wilson and Gravelle (1991) was assigned as an input in the model.

3.2.2 Towers

The towers were modelled using linear elastic beam elements (Fig. 3.10). In total, three cross sections were assigned along the height of each leg in accordance with the geometry presented in Fig. 3.4. More specifically, nine elements were defined in the leg below the deck with the geometry of Section 1-1, i.e., one element between deck and lower strut, and eight equal-length elements below the lower strut in Z direction. One element (i.e., element #10) is assigned over the region having the properties of Section 2-2, and one element with properties of Section 3-3 is defined to connect the center of the upper strut and the end node of the element #10. The leg above the upper strut is modelled with one element, where a joint is added at each location for cable anchor. As presented in Fig. 3.10, the upper strut is modeled as one beam element while the lower strut is modelled using ten elements. Given the above, each tower was modelled with thirty-five beam elements. The solid concrete wall below the lower strut was modelled as a shell element and meshed into 8x8 sub elements to achieve a higher accuracy of the results.

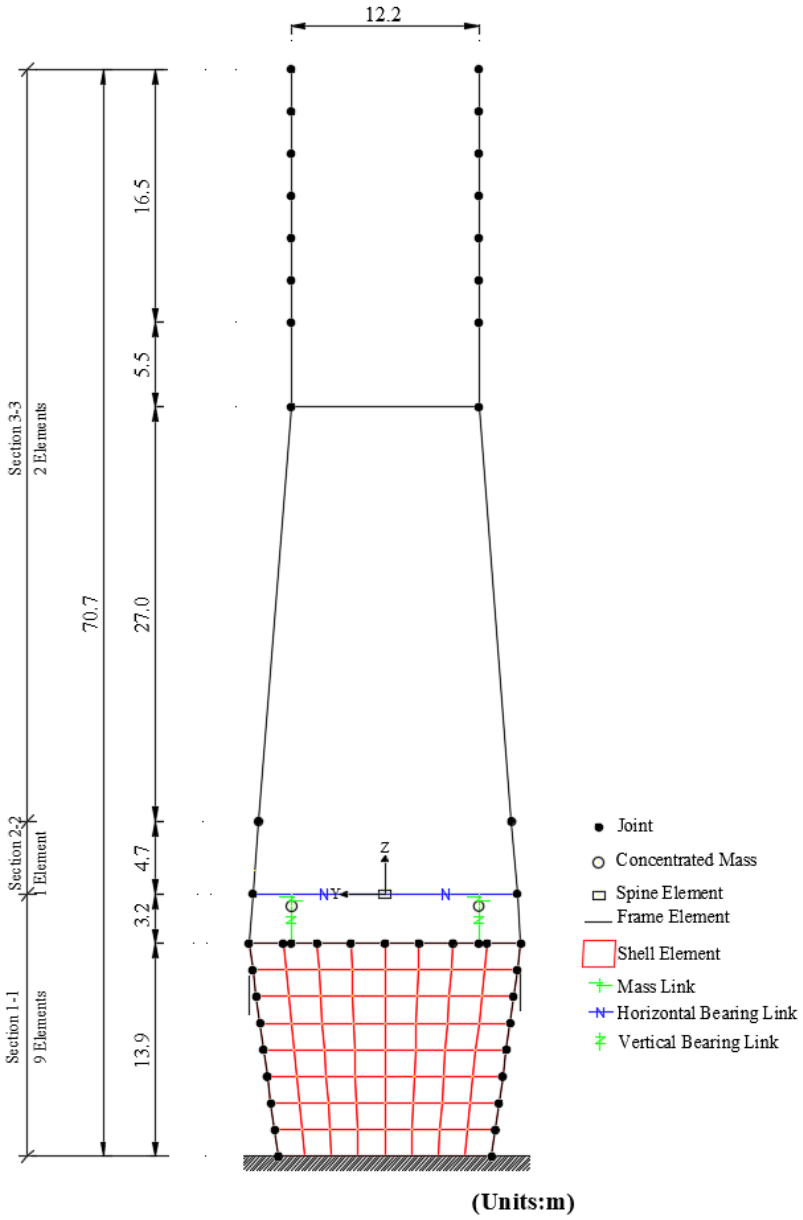

Figure 3.10 Finite element model of the tower.

3.2.3 Cables

As discussed in Chapter 2, Section 2.3 one of the sources leading to nonlinearity of cable-stayed bridges is cables, whose nonlinear behaviour can be represented by the modified modulus of elasticity of the cable. However, Hua and Wang (1996) reported that

using modified modulus of elasticity of cables only produced 2% difference on modal frequencies compared to using original modulus of elasticity without considering nonlinearity of cables. Furthermore, they concluded nonlinear effects on cables could be ignored on the analysis of Bayview Bridge. Given this, each cable was modeled using "Straight frame object (cable)" in SAP2000, i.e., one linear segment without sag. Four cable sections (i.e., Labels 1, 2, 3, and 4 in Fig. 3.11) were used to model the total 56 cables.

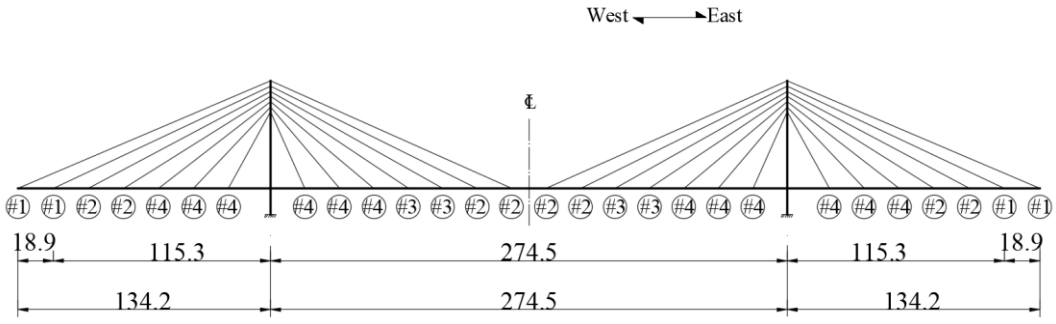

Figure 3.11 Layout of cable sections adopted from Wilson and Gravelle (1991) (units: m).

3.2.4 Bearings

The vertical bearings at both towers are fixed in the vertical direction. The horizontal bearings restrict the transverse displacement, i.e., the three translational degrees of freedom of these bearing are considered to be fixed. Regarding the rotational behaviour of the bearings, all the deck/tower bearings allow the relative rotation only about y-axis, i.e., rotations about x- and z-axes are not allowed.

As illustrated in Fig. 3.10, bearings are modeled using two horizontal and two vertical links at each tower. The horizontal ones are used to simulate the bearings that connect the deck to the tower legs. The vertical ones are used to model the vertical bearings

to connect the deck with the lower strut. The degrees of the freedom of these links are defined in such a way that only the rotation about y-axis is allowed and the other five degrees (three translation and two rotation) are restricted.

3.2.5 Foundation and boundary conditions

The tower bases were considered to be fully fixed in all the six degrees. Given the mechanism of the connection between the deck and the abutment as described in Section 3.1, the joint at each end of the bridge was assigned with following boundary conditions,

- Rotation about y- and z -axes is free
- Rotation about x-axis is restrained
- Translation in all three directions is restrained.

3.2.6 Damping

Pridham and Wilson (2005) evaluated the damping of the Quincy Bayview Bridge based on extensive data collected during the ambient vibration tests conducted in 1987. They reported that the damping of the first vertical mode of the bridge was about 1.4%, and that of the first transverse-torsional mode was about 1.1%. Furthermore, they suggested that an average damping of 1.0% with a standard deviation of ±0.8% could be assigned to all the modes. Following their suggestion, in this study a damping of 1.1% was assigned to all the modes except the first vertical mode where a 1.4% damping was considered.

3.3 Modal validation

In order to validate the finite element model developed in this study, the dynamic characteristics of the bridge from the current study were compared with those provided in

Wilson and Gravelle (1991) and Wilson and Liu (1991). For ease of discussion, the results from the current study, Wilson and Gravelle (1991) and Wilson and Liu (1991) are referred to as CFEM (**C**urrent **F**inite **E**lement **M**odel), Wilson FEM and Wilson Test, respectively. The parameters for comparison are mode shape and modal frequency. It should be noted that comparison of mode shapes was conducted graphically, i.e., not point-to-point comparison was checked out. This is because Eigenvalues shown in all figures in this section with *label b* were not available.

3.3.1 Modal shapes

Vertical modes

Figure 3.12a presents the vertical mode shapes provided by CFEM, and Figure 3.12b illustrates the results from Wilson FEM and Wilson Test as reported in Wilson and Liu (1991). In Fig. 3.12 and all similar figures hereafter such as Figs. 3.13 and 3.14, the horizontal axis represents the distance along the deck measured from the bridge west end, and the vertical axis demonstrates the normalized Eigen values to the maximum of 1.0.

It can be seen clearly in Fig. 3.12 that the mode shapes from CFEM and Wilson FEM are almost identical. This is due to the fact that the CFEM model was developed following the same techniques for Wilson FEM model as explained in Wilson and Gravelle (1991). By comparing CFEM results with Wilson Test results, it is noticed that they are very similar for the first six modes. A minor difference is observed in the 7^{th} and 8^{th} modes; however, the difference is only limited within the main span. Such difference might be due

to the length of the segments defined in modelling, i.e., using only one element to connect the anchorages between two cables would not be able to consider the effect of curvature of the deck as reported in Wilson and Liu (1991).

(a) (b)

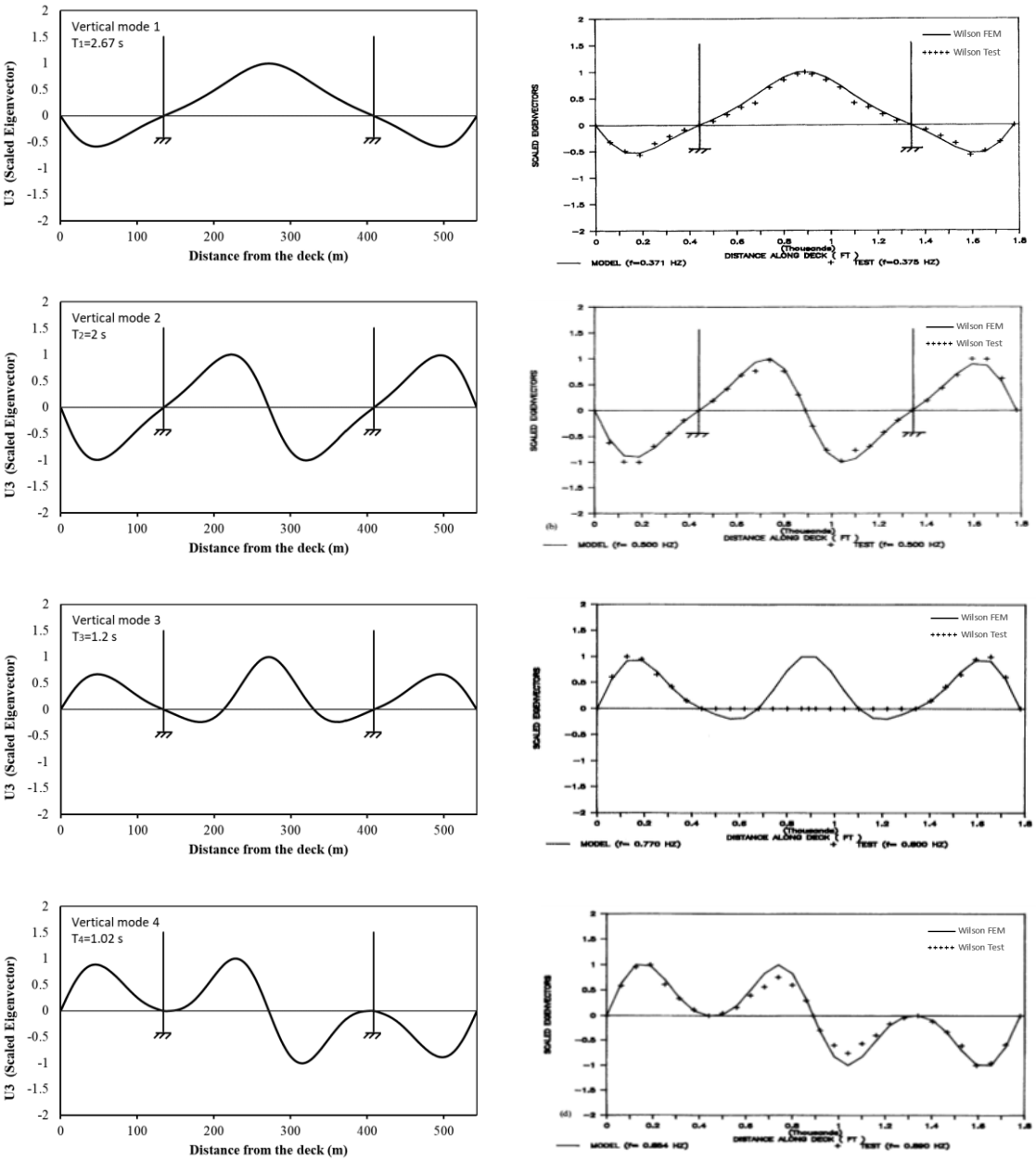

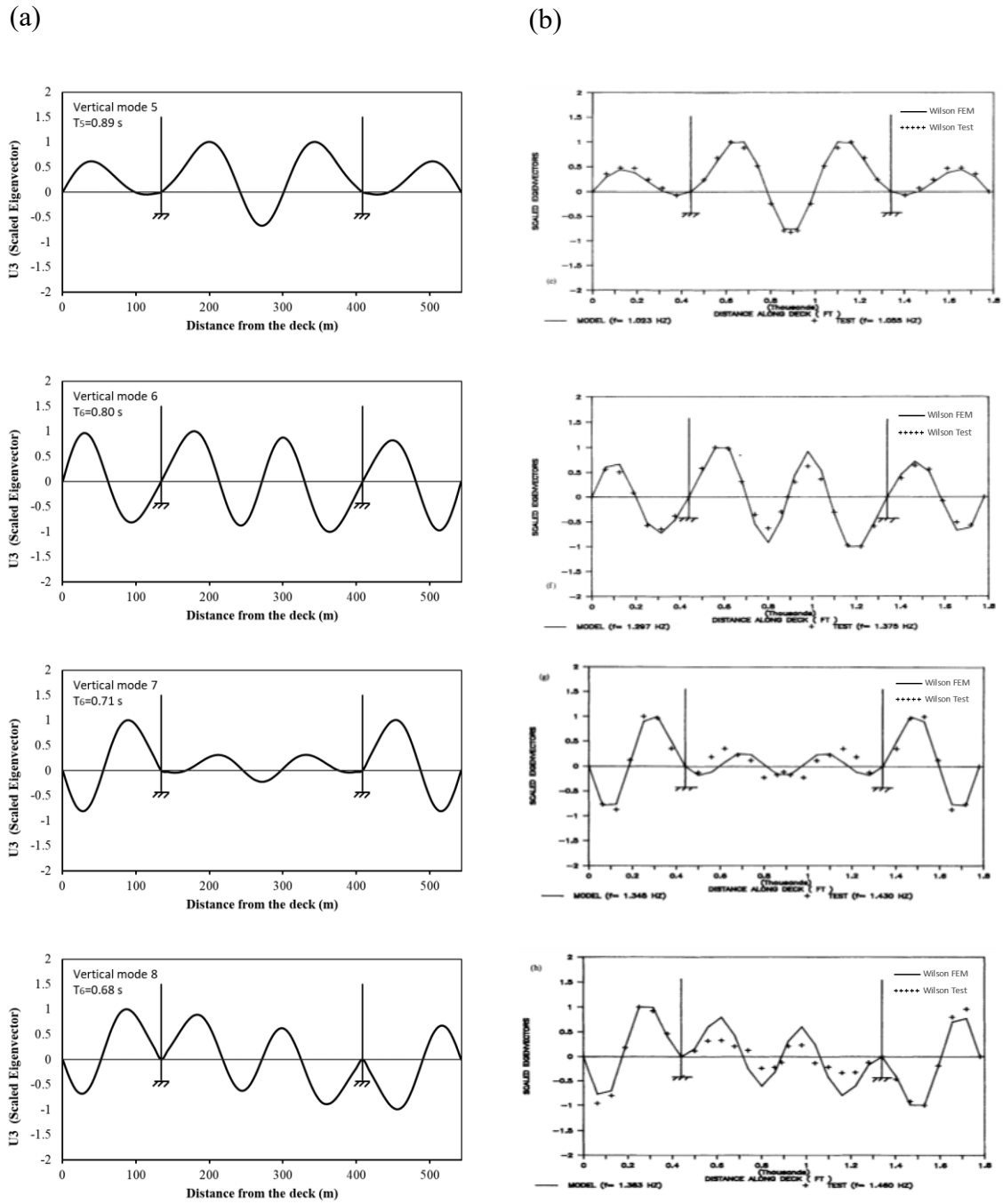

Figure 3.12 Comparison of vertical mode shapes: (a) CFEM results; (b) Wilson FEM and Wilson Test results.

Torsional modes

The results for torsional modes (Fig. 3.13) show that the CFEM and Wilson FEM provide almost the same mode shapes except for the 2nd mode. With respect to the 2nd mode, the Eigen values of the vibration in the two side spans obtained from CFEM are almost two times those from Wilson FEM. However, for the main span, the mode shape shown in CFEM consists of three segments while there is only one segment in Wilson FEM. It is necessary to mention that for the 4th mode, the amplitudes of the motion in the main span from Wilson Test are shown as zero. This is because the data was not collected during the ambient tests due to technical issues as reported in Wilson and Liu (1991).

(a) (b)

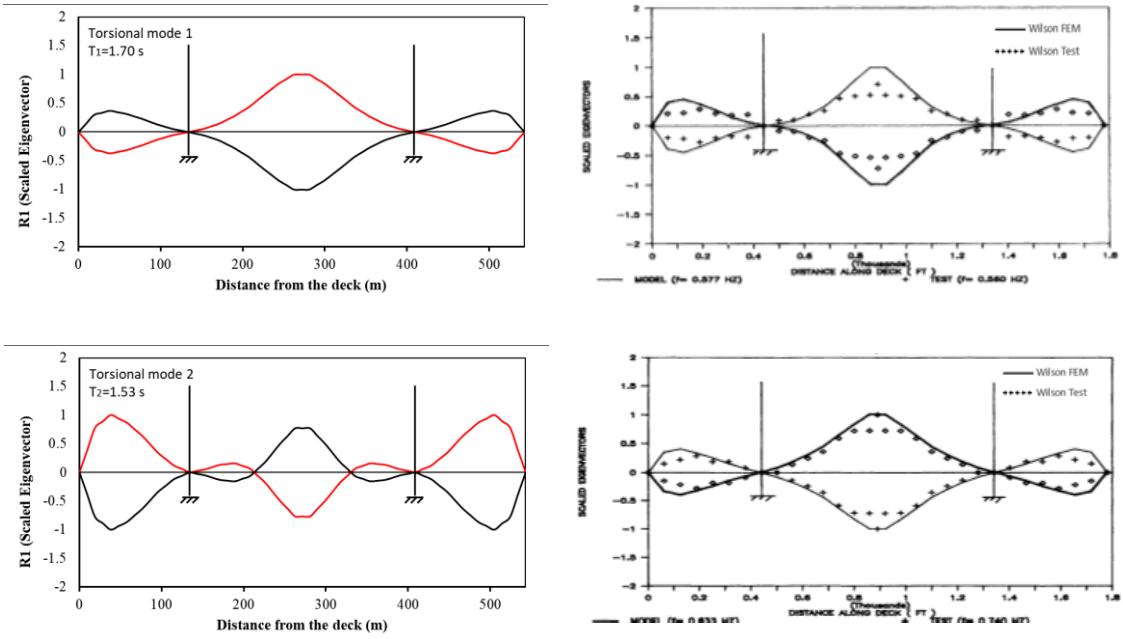

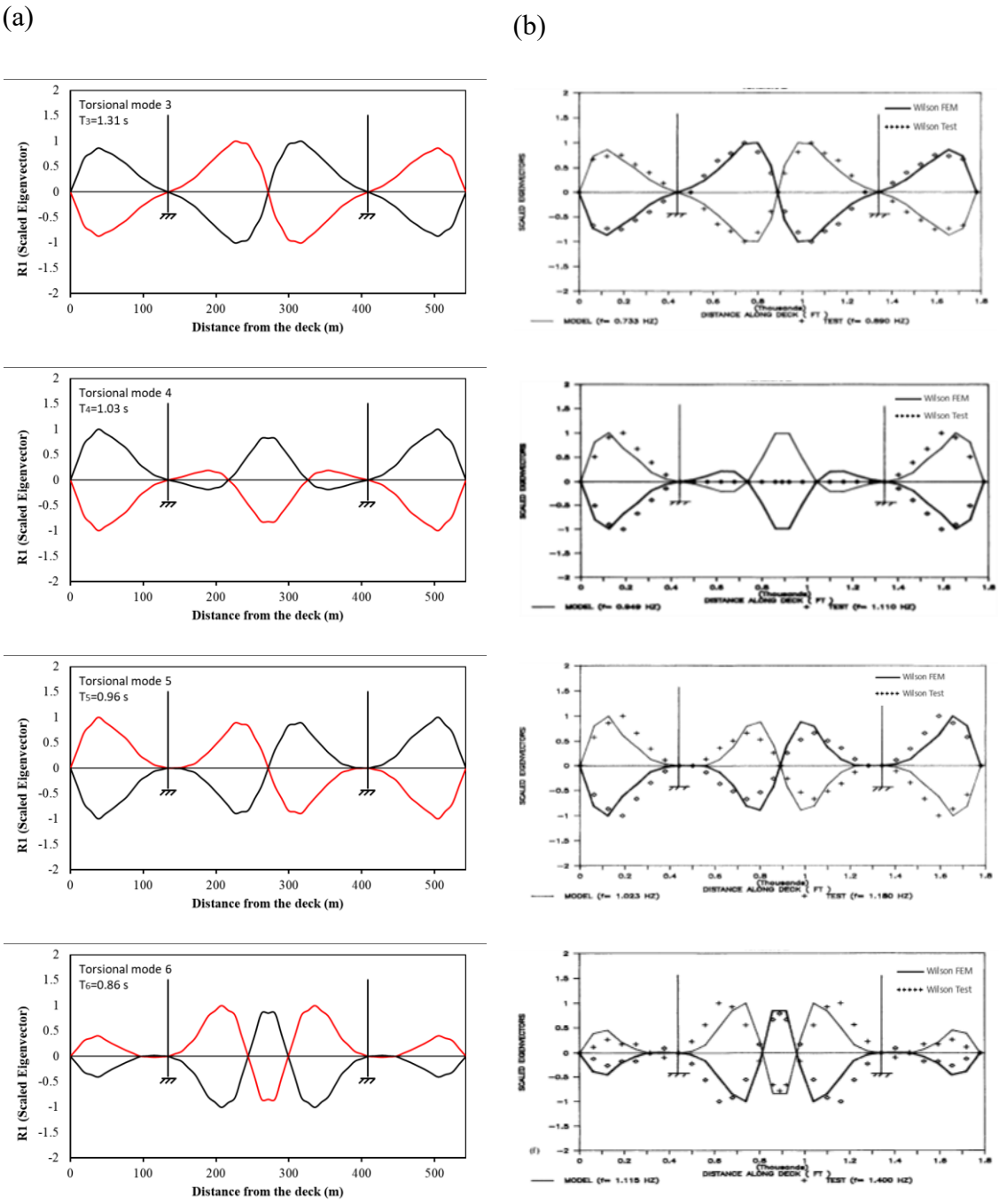

Figure 3.13 Comparison of torsional mode shapes: (a) CFEM results; (b) Wilson FEM and Wilson Test results.

Transverse modes

Figure 3.14 illustrates the mode shapes in the transverse direction given by CFEM (Fig. 3.14a), and Wilson FEM and Wilson Test (Fig. 3.14b). It can be seen clearly in the figure that five out of total six transverse modes provided by CFEM have a similar shape to those given by Wilson Test. It can be concluded that the model developed in this study CFEM is much better than Wilson FEM in predicting the transverse modes, since only the first two mode shapes (1st and 2nd) from Wilson FEM are compatible with Wilson Test. By comparing the results given in Figs. 3.12 and 3.13, it is noticed that the bridge vibration is dominated by the torsional modes not the translation modes.

(a) (b)

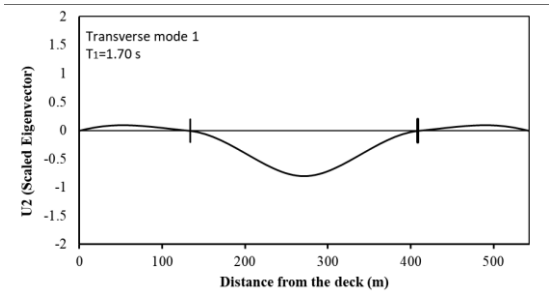

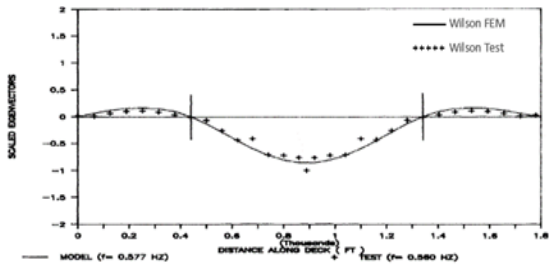

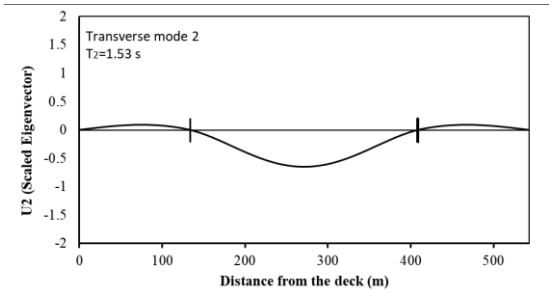

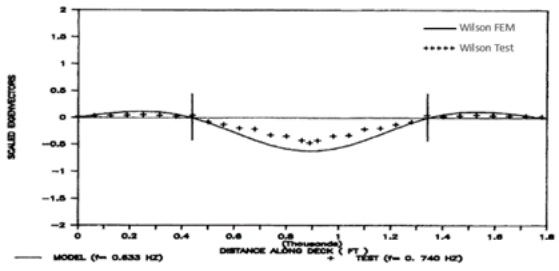

(a) (b)

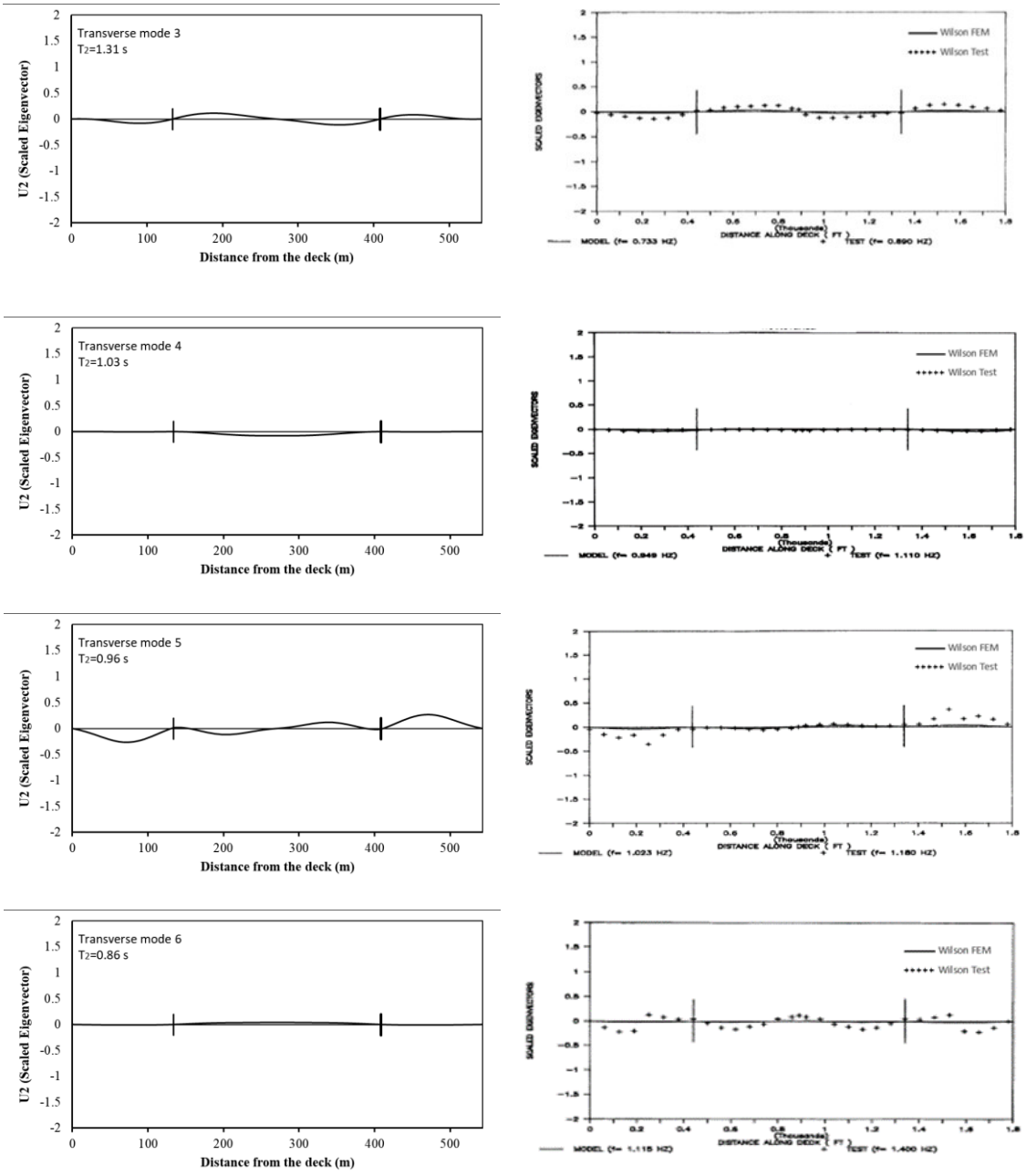

Figure 3.14 Comparison of transverse mode shapes: (a) CFEM results; (b) Wilson FEM and Wilson Test results.

3.3.2 Modal frequencies

The results for frequency from CFEM, Wilson FEM, and Wilson Test are presented in Fig. 3.15. It can be in the figure that, for the first five modes, the frequencies from these three studies match very well. However, the difference becomes noticeable for some higher modes, such as, Mode 12, Mode 14 and Mode 15. Table 3.2 provides the frequencies of the 17 modes obtained from CFEM, Wilson FEM and Wilson Test for purpose of comparison and validation of the model. For ease of understanding, the difference on the frequencies between each of Wilson FEM and Wilson Test associated with CFEM is presented in the table, i.e., the amount given in the bracket. It can be seen in the table that the maximum difference in these two cases is only about 0.13Hz (Mode 15). Such results indicate the model developed in current study CFEM is acceptable for further time-history analysis to examine bridge responses. It is necessary to mention that the frequency for Mode 12, 14 and 15 are not provided by Wilson FEM.

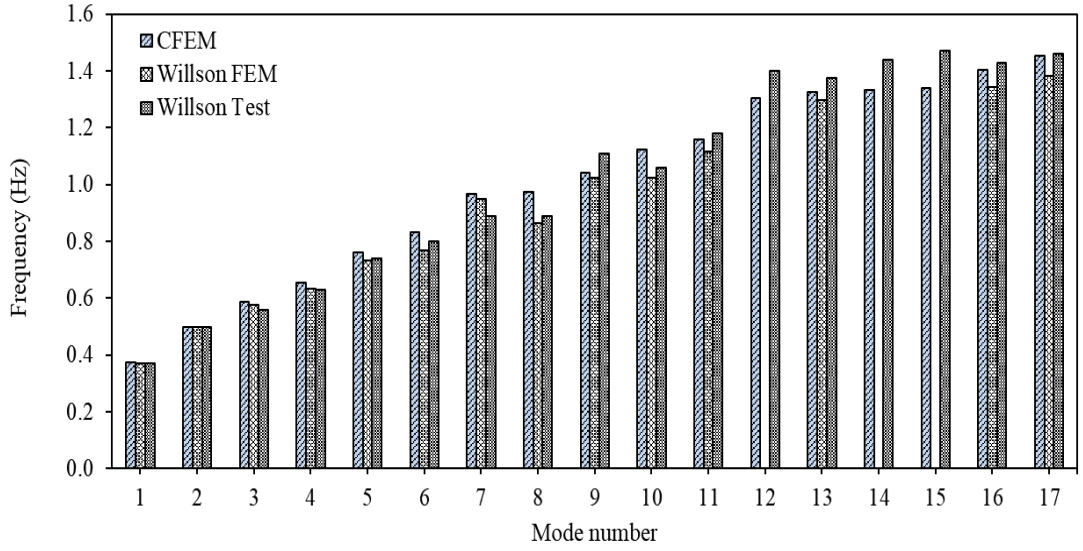

Figure 3.15 Modal frequencies from CFEM, Wilson FEM and Wilson Test.

Table 3.2 Modal frequencies.

Direction of vibration	Frequency (Hz)		
	CFEM	Wilson FEM	Wilson Test
Vertical	0.374	0.371 ***(0.003)****	0.370 ***(0.004)***
Vertical	0.498	0.500 ***(-0.002)***	0.500 ***(-0.002)***
Torsional -Transverse	0.587	0.577 ***(0.010)***	0.560 ***(0.027)***
Torsional -Transverse	0.654	0.633 ***(0.021)***	0.630 ***(0.024)***
Torsional -Transverse	0.760	0.733 ***(0.027)***	0.740 ***(0.020)***
Vertical	0.833	0.770 ***(0.063)***	0.800 ***(0.033)***
Torsional -Transverse	0.966	0.949 ***(0.017)***	0.890 ***(0.076)***
Vertical	0.973	0.864 ***(0.109)***	0.890 ***(0.083)***
Torsional -Transverse	1.041	1.023 ***(0.018)***	1.110 ***(-0.069)***
Vertical	1.122	1.023 ***(0.099)***	1.060 ***(0.062)***
Torsional -Transverse	1.158	1.115 ***(0.043)***	1.180 ***(-0.022)***
Torsional -Transverse	1.305	NA	1.400 ***(-0.095)***
Vertical	1.327	1.297 ***(0.030)***	1.375 ***(-0.048)***
Torsional -Transverse	1.333	NA	1.440 ***(-0.107)***
Torsional -Transverse	1.340	NA	1.470 ***(-0.130)***
Vertical	1.403	1.345 ***(0.058)***	1.430 ***(-0.027)***
Vertical	1.452	1.383 ***(0.069)***	1.460 ***(-0.008)***

* The number in bracket provides the difference between the result from CFEM and the reference. The positive number indicates the CFEM frequency is higher.

Chapter 4

ANALYSIS RESULTS

4.1 Selection of records

For the purpose of seismic analysis, ten records were selected from Strong Ground Motion Database developed by Pacific Earthquake Engineering Research Center (PEER). Characteristics of the records selected are presented in Table 4.1. Among the ten records, eight of them were selected from the most devastating earthquakes in the United States. It can be seen in the table that two records from earthquakes in Asia, i.e., Kobe earthquake and Chi Chi earthquake, were also selected for the analysis. This is because these earthquakes were considered as the most significant earthquakes occurred in recent years. Among the three components of each record, the horizontal component with a larger PGA was chosen while the vertical component was not considered given the objective of the study. More specifically, the magnitude of the earthquakes is between 5.99 and 7.62, the PGA of the records ranges from 0.11 g to 0.69 g with an average of about 0.29 g, and the PGD is from 10 mm to 255 mm with an average of about 88 mm. The total duration of the ground motion for the records is between 28.34 s to 89.99 s. It is necessary to mention herein that the PGD of Re #1 (14 mm) from Whittier earthquake and Re #6 from Kobe earthquake (10 mm) is relatively small compared with the other records. They were selected to demonstrate that seismic excitation with low displacement might also have potential to trigger resonance in bridge vertical direction when multi-support excitation is

considered in the seismic analysis. Since the purpose of this study is not to evaluate the demand for the design of the Bayview Bridge, the selected records are not site-specific and are not scaled to match the design-spectrum for the bridge. Figure 4.1 presents the acceleration time-history and the displacement time-history of each record based on the data downloaded from PEER database.

Table 4.1 Characterises of the records.

Record ID	Earthquake Name	Station	Mag. (M)	Dis. (km)	Comp. (Deg.)	PGA (g)	PGD (mm)	Duration (s)
Re #1	1987 Whittier	Studio City	5.99	26.91	182	0.23	14	32.39
Re #2	1984 Morgan Hill	Gilory Array # 4	6.19	11.53	360	0.34	33	39.99
Re #3	1979 Imperial Valley	Superstition Mtn Camera	6.53	24.61	135	0.20	27	28.34
Re #4	1971 San Fernando	Santa Felita Dam	6.61	24.69	172	0.15	92	39.99
Re #5	1994 Northridge	Castiac-Old Ridge Route	6.69	20.11	090	0.56	95	39.98
Re #6	1995 Kobe	Chihaya	6.90	49.91	090	0.11	10	53.99
Re #7	1989 Loma Prieta	Palo Alto-SLAC Lab	6.93	30.62	360	0.27	115	39.64
Re #8	1992 Landers	Barstow	7.28	34.86	000	0.13	146	39.98
Re #9	1952 Kern County	Taft Lincoln School	7.36	38.42	111	0.18	93	54.36
Re #10	1999 Chi Chi	TCU095	7.62	45.15	N	0.69	255	89.99

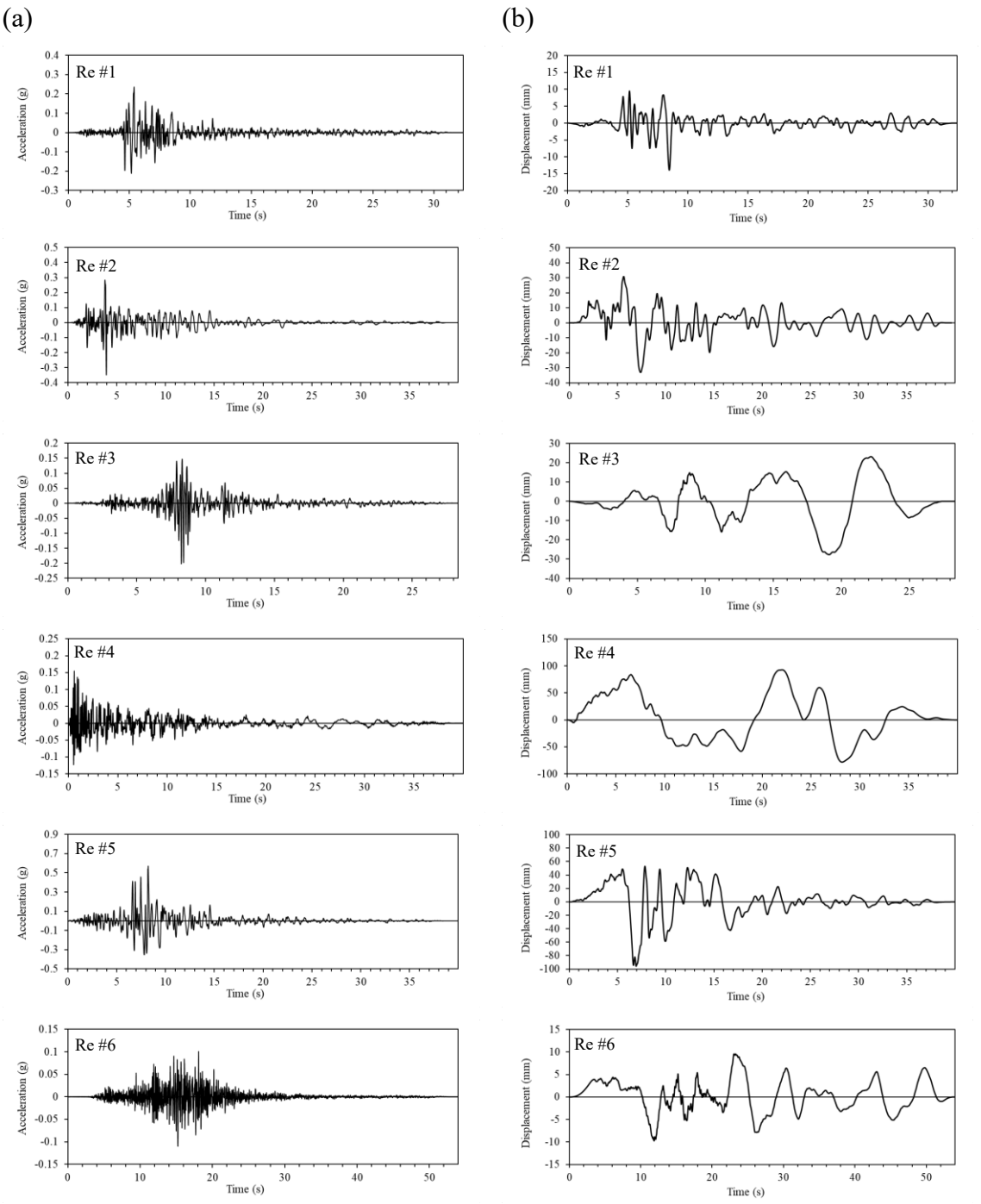
(a)
(b)
Re #1
Re #2
Re #3
Re #4
Re #5
Re #6
Acceleration (g)
Displacement (mm)
Time (s)

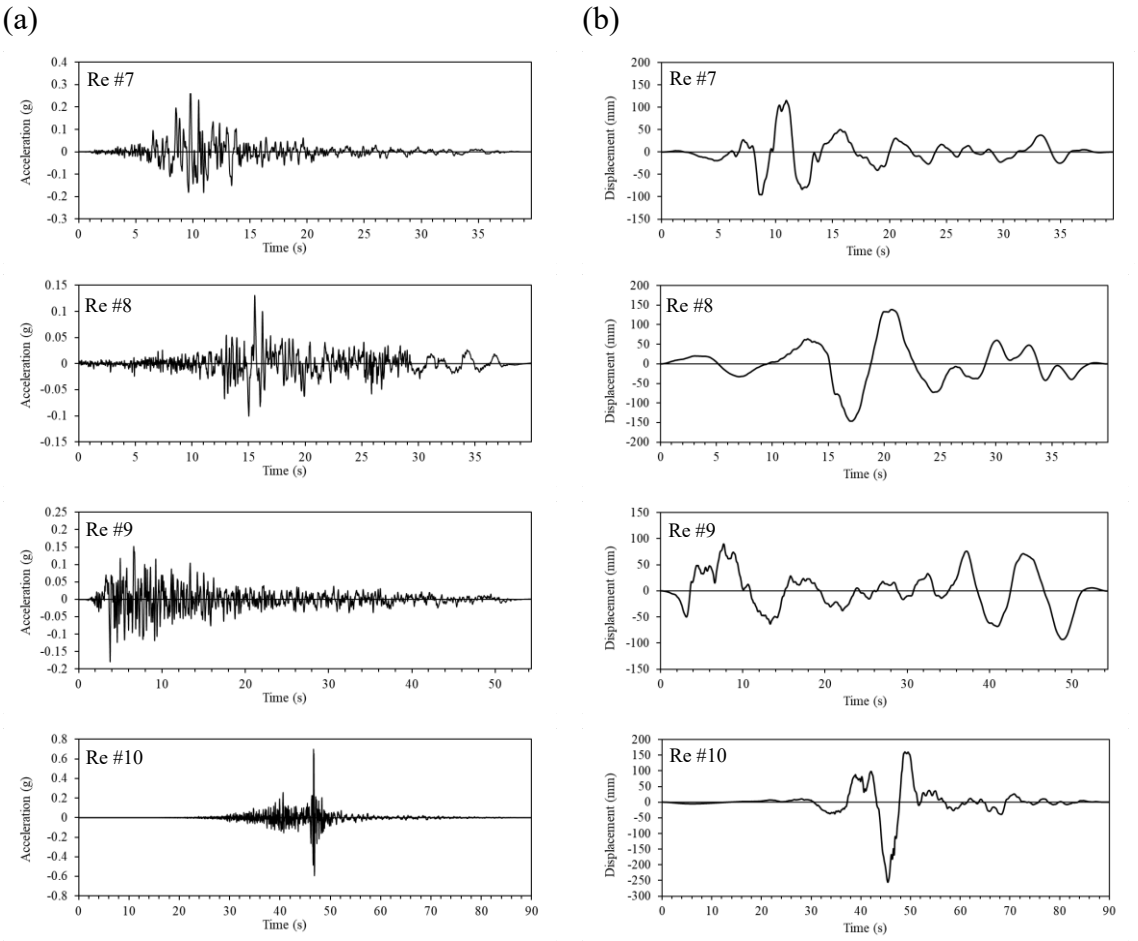

Figure 4.1 Time-histories of the records: (a) acceleration; (b) displacement.

4.2 Preliminary investigation into bridge response due to multi-support excitation

As discussed in Chapter 2, this study focuses on the phase delay on the ground motion assigned at each support in a long-span bridge. Given this, a preliminary analysis was conducted on the model of the Bayview Bridge subjected to non-uniform excitation, which is designated as loading case MSE (**M**ulti-**S**upport **E**xcitation) hereafter for simplicity. The displacement at the middle of the second span (i.e., Joint 29 in SAP model,

Fig. 4.2) and at 36.6 m from the center of the bridge (i.e., Joint 33 in SAP model) was chosen to examine the effect of MSE on the bridge response. These two locations were selected as Joint 29 represents the node where the displacement in vertical direction (i.e., Direction Z, Fig. 4.2) is maximum due to MSE. Joint 33 represents the node where the displacement in the vertical direction is maximum when the same excitation is applied at each support, supports 1, 2, 3, and 4, in which is this loading case is referred to as Uniform.

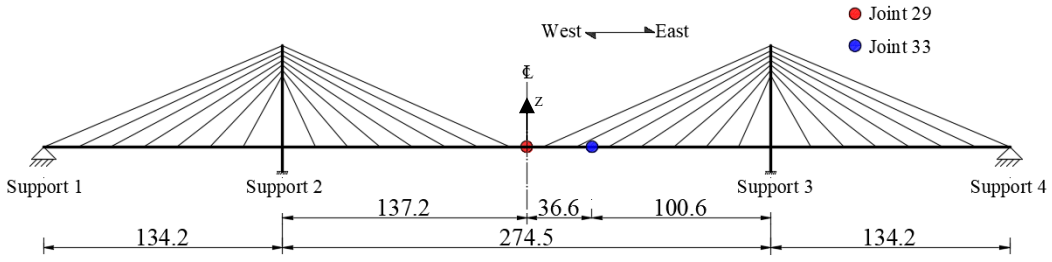

Figure 4.2 Elevation view of the Bayview Bridge.

To generate the excitation time-history to be applied at each support due to time delay for MSE loading case, the delayed time of seismic wave travelling from one support to another must be determined first. In this preliminary analysis, the lower bound of the shear wave velocity for Soil Class D defined in CHBDC (i.e., 185 m/s) was assumed in the calculation. Assuming the wave starts at support 1 and travels to the east, then the time delay at supports 2, 3, and 4 with respect to support 1 is about 0.72 s (= 134.2/185), 2.21 s (= 408.7/185), and 2.93 s (= 542.9/185). Then the time-history of the ground motion at each of these supports, i.e., support 2, support 3, and support 4, can be derived (Christian 1976). As an example, Figure 4.3 shows the displacement time histories from Loma Prieta Earthquake (i.e., Re #7, Table 4.1) to be assigned at the supports in the bridge model. It is

necessary to mention that the decay of the ground motion amplitude through travelling is neglected in this study.

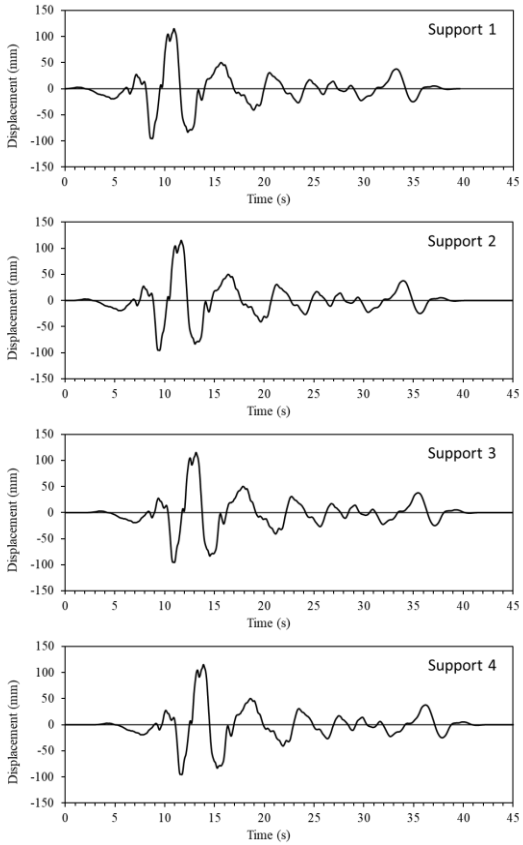

Figure 4.3 Phase-delayed time-history at each bridge support, Re #7, wave velocity of 185 m/s.

Once the displacement time series at the four supports from each record are generated, they are assigned in the longitudinal direction in the bridge model for seismic analysis. The maximum absolute displacements from each record for Joints 29 and 33 were extracted from SAP2000 and are presented in Figs. 4.4 and 4.5, respectively. For comparison purpose, the results from the uniform loading are also presented in Fig. 4.4 and

4.5. In the case for uniform loading, the original displacement time-history of each record as presented in Fig. 4.1 is assigned at all four supports. The major observations from the results are summarized as follows,

For the Uniform loading case

- No vertical displacement is triggered at Joint 29,
- Vertical displacement is triggered at Joint 33, in which the maximum among the 10 records is about 183 mm from Northridge earthquake,
- The longitudinal displacement at Joints 29 and 33 is almost identical. This besides the maximum displacement at the two joints is compatible.

For the MSE loading case

- Significant vertical displacement is triggered at both Joints 29 and 33, which is much higher than that obtained from the Uniform loading case.
- As discussed in Section 4.1, the PGD of Re #6 from Kobe Earthquake is 10 mm (Table 4.1). However, the maximum vertical displacement at Joint 29 has reached about 85 mm, which is about ten times the response from the Uniform loading case. Accordingly, attention should be paid to as seismic ground motion with low PGD that might cause relatively high vertical displacement if MSE is considered in the analysis.
- The longitudinal displacement is smaller than that from the Uniform loading case. This is consistent with the finding reported in Zerva (1991). According to Zerva, when the seismic excitation is applied in the bridge longitudinal

direction and when the multi-support excitation is considered, the longitudinal displacement obtained is expected to be smaller than that when the multi-support excitation is ignored, i.e., uniform excitation.

The most interesting finding from the results shown in Figs. 4.4 and 4.5 is that, vertical displacement is much larger than the longitudinal displacement when MSE is considered. This could lead to a more general statement that the displacement in the direction orthogonal to the loading direction is larger than the response associated with the direction where the earthquake load is applied. However, most of previous studies used the displacement in the direction of loading as a response parameter to evaluate the performance of long-span structures under multi-support excitation (Zerva 1991; Li and Li 2004; Crewe and Norman 2006; Aswathy et al. 2013). To be more precise, the response in the orthogonal direction, i.e., vertical direction, was ignored in the past studies.

Given this, detailed analyses were conducted in this study to examine the response of the Bayview Bridge in vertical direction due to the seismic loading in the horizontal direction, as described in following sections.

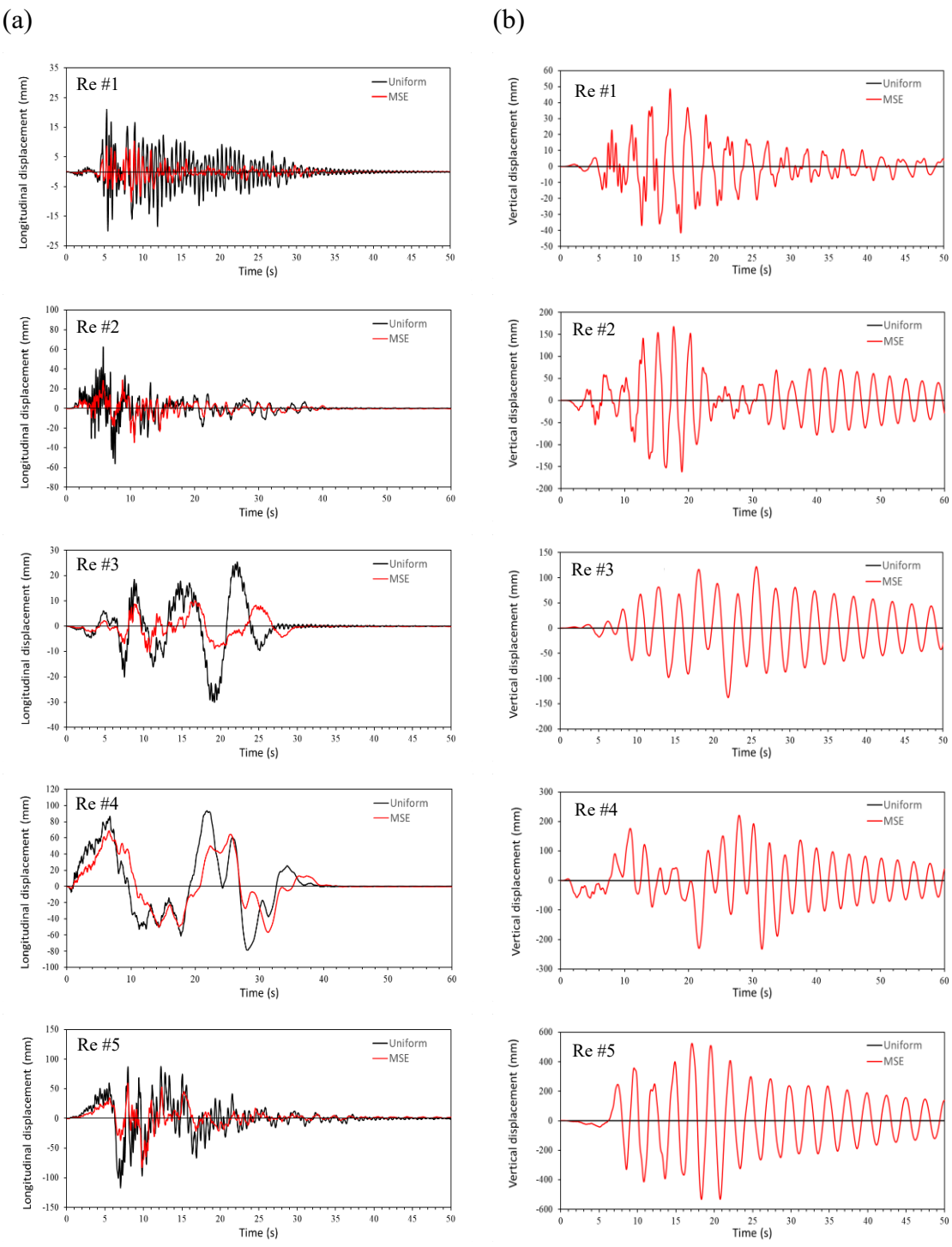
(a)
(b)
Re #1
Re #2
Re #3
Re #4
Re #5
Uniform
MSE
Longitudinal displacement (mm)
Vertical displacement (mm)
Time (s)

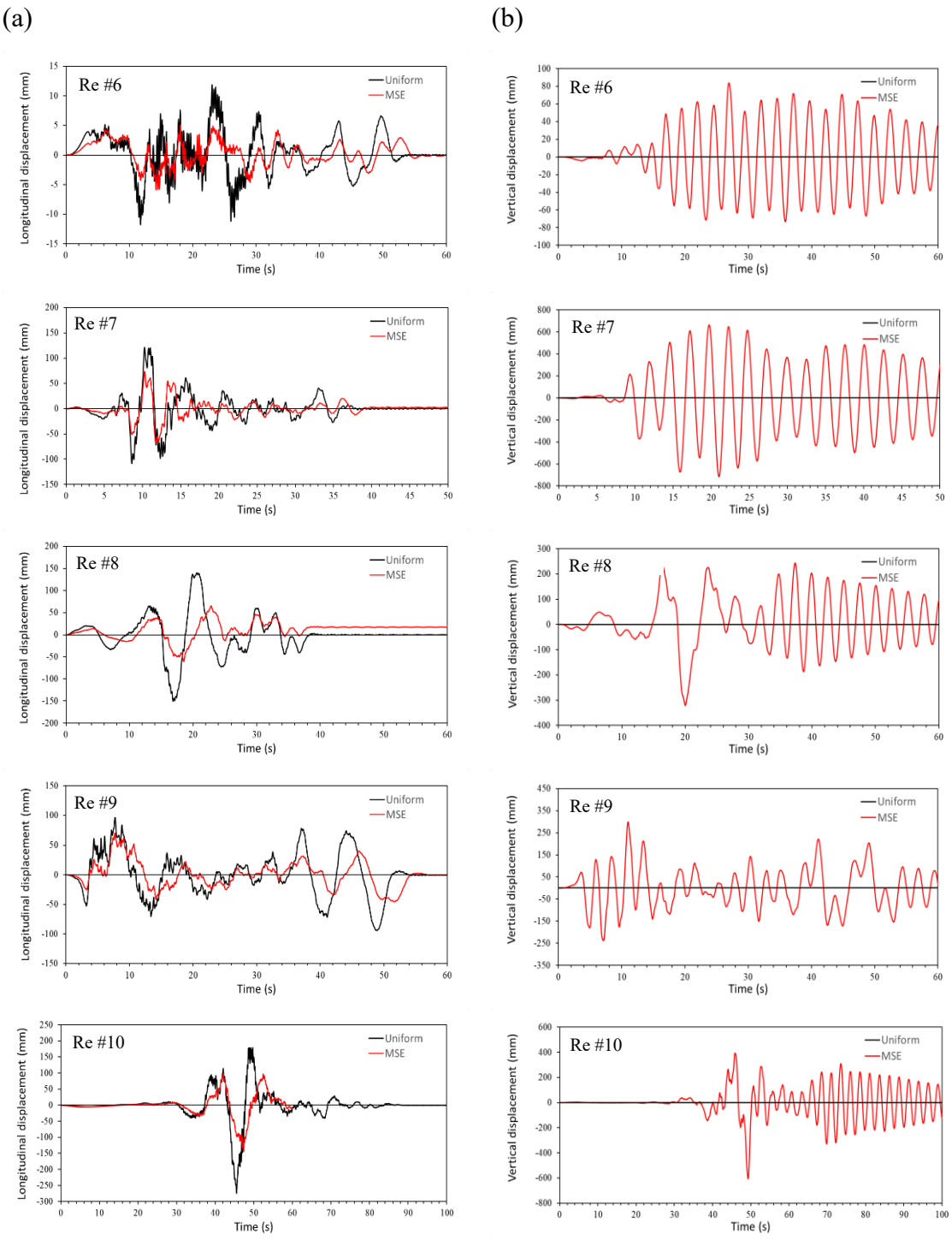

Figure 4.4 Absolute displacement at Joint 29: (a) Longitudinal; (b) Vertical.

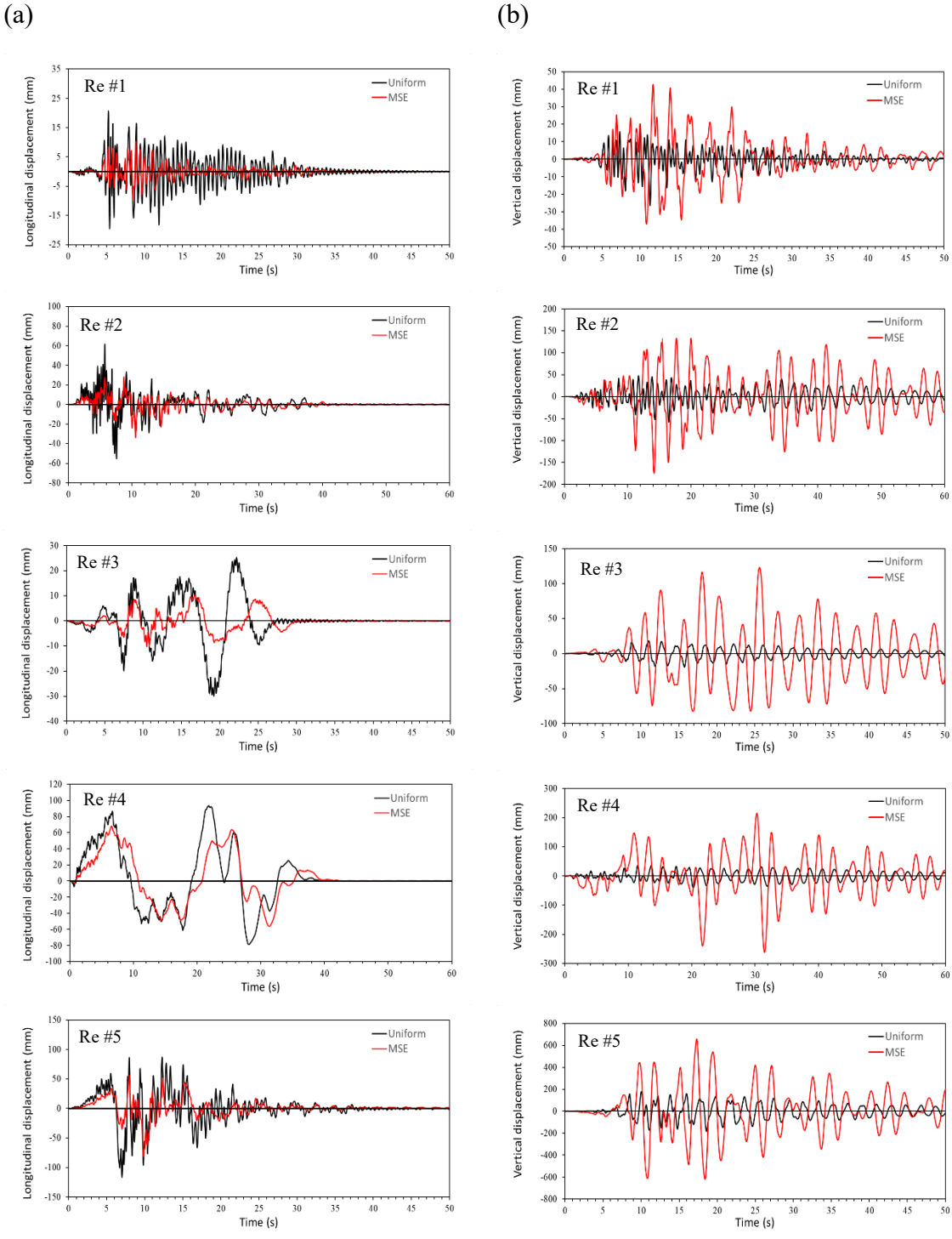
(a)
(b)
Re #1
Re #2
Re #3
Re #4
Re #5
Uniform
MSE
Longitudinal displacement (mm)
Vertical displacement (mm)
Time (s)

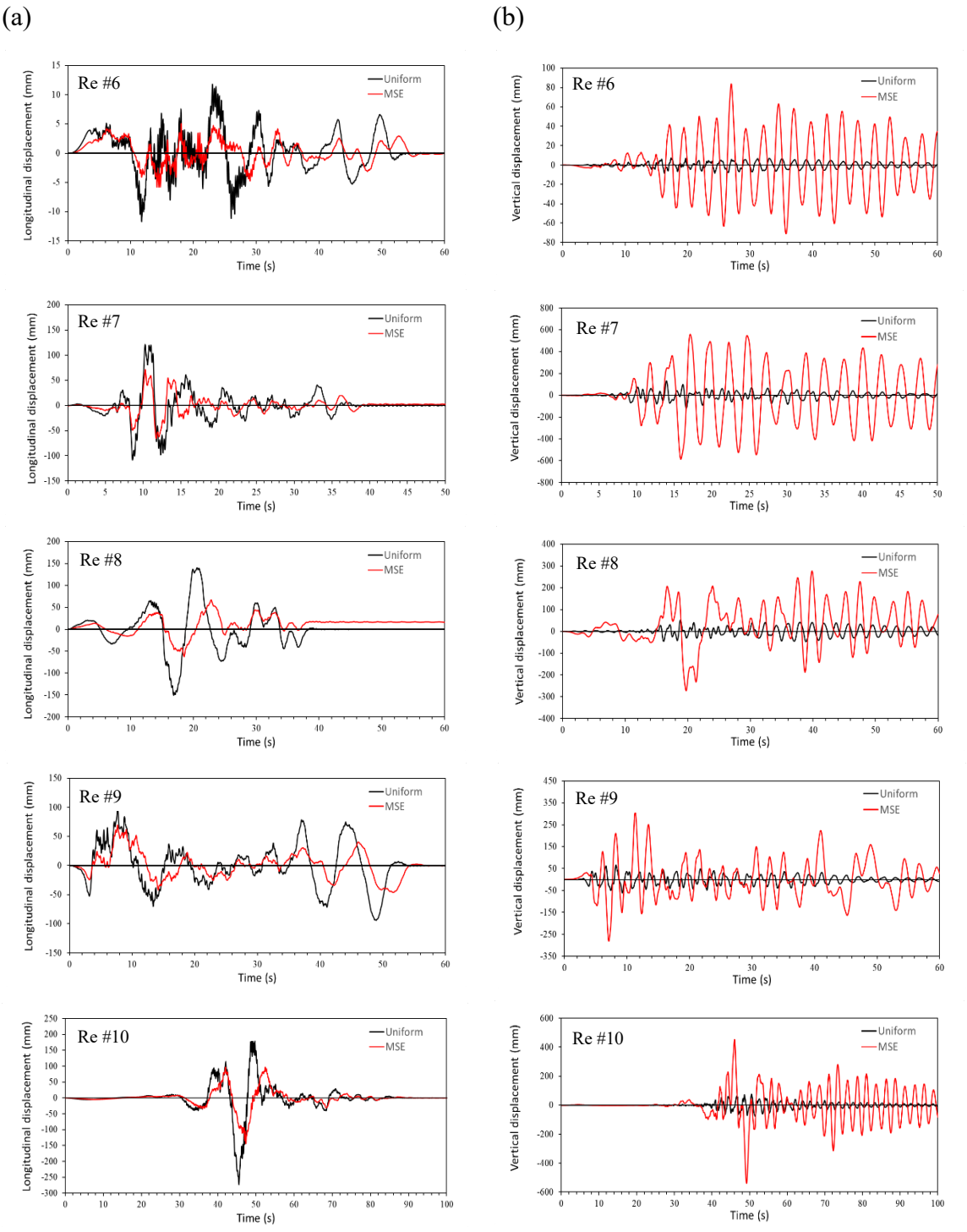

Figure 4.5 Absolute displacement at Joint 33: (a) Longitudinal; (b) Vertical.

4.3 Understanding structural response in vertical direction

To understand the response of Bayview Bridge in vertical direction due to seismic excitation applied in longitudinal direction considering MSE, a generic one bay one storey 2D frame was created in SAP2000 (Fig. 4.6). The span length of the frame is 7.3 m, the height is 3.6 m. As shown in Fig. 4.6, a lumped mass is added at the center of the beam, i.e., 453.6 kg for horizonal direction, 226.8 kg for vertical direction. In the modeling, both beam and columns are massless and their axial stiffness is assigned to be infinite. Stiffnesses for columns and beam are 3245.7 kN/m and 3219.5 kN/m, respectively. These values were chosen in such a way that, (i) the period of the mode in the horizontal and vertical direction is governed by the lumped mass only; (ii) the periods are suitable for the purpose of the investigation to be conducted, i.e., they both are not too short and they are far apart; (iii) the vertical mode and the horizontal mode are not coupled. The results from the SAP2000 modal analysis provide the period of mode 1 T_{n1} = 2.35 s (horizontal mode), mode 2 T_{n2} = 1.67 s (vertical mode). The subscript *"n"* stands for the Natural period of the structure.

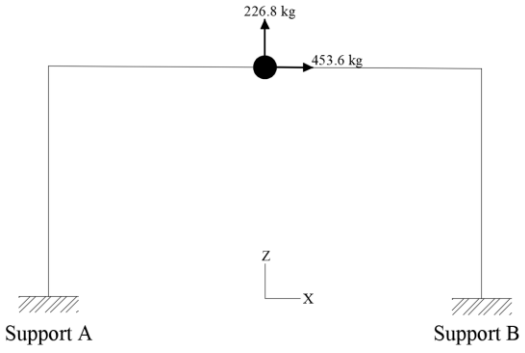

Figure 4.6 Elevation view of the generic 2D frame

Two loading cases were considered, i.e., one is the Uniform loading, the other is MSE. In both cases, the excitation is applied in the frame longitudinal direction, i.e., X direction in Fig. 4.6. The ground motion excitation is represented by a sinusoidal function as any ground motion time-history can be represented by a sum of sinusoidal functions with different amplitude and phase angle. The amplitude of the function is assumed to have a constant peak of 25 mm. However, the period of the input function T_g is a variable, in which the subscript g stands for **G**round motion. For the case of MSE, the delayed time T_d is also a variable, in which the subscript *"d"* stands for **D**elay. The reason why both T_g and

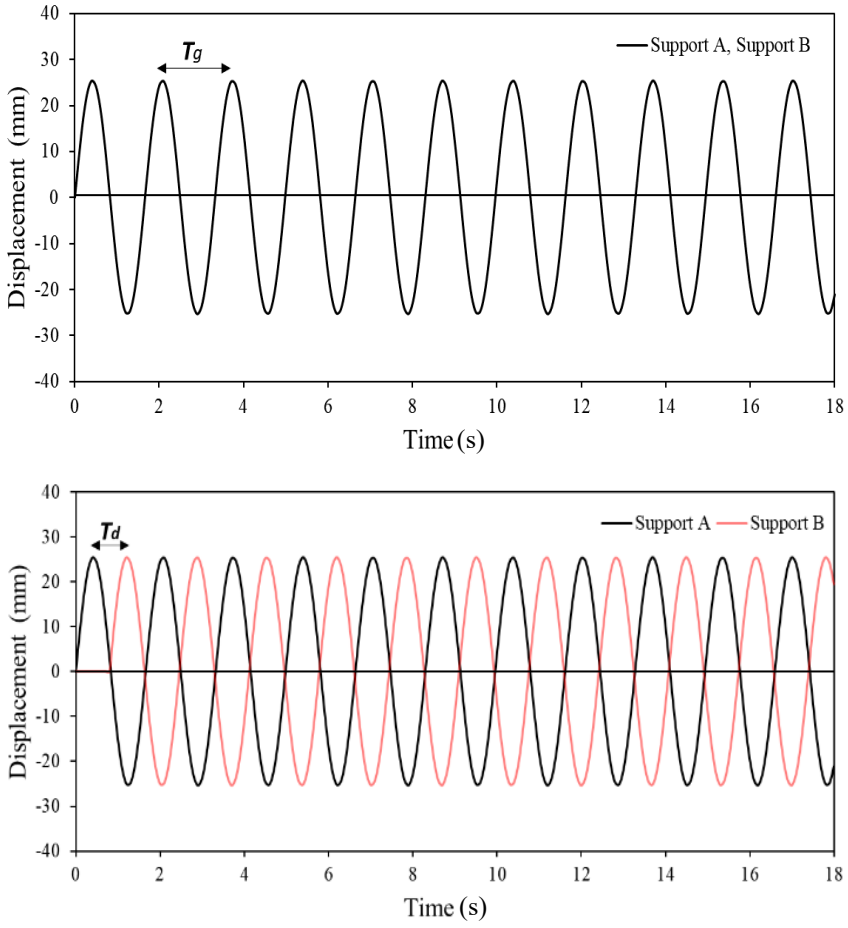

Figure 4.7 Artificial excitation for testing: (a) Uniform loading case; (b) MSE loading case.

T_d are a variable instead of constant is because of the purpose of the investigation, namely, to understand a specific condition that the maximum displacement of the mass could be generated. As an example, Figures 4.7a and 4.7b present the excitation for the Uniform loading case and MSE case, respectively for a given T_g = 1.67 s, T_d = 0.83 s.

A number of analyses were conducted for different pairs of T_g and T_d. It was found that, for the uniform loading case, the maximum displacement (about 252 mm, 5% damping) for the mass in the longitudinal direction was obtained when T_g = 2.35 s equal to the period T_{n1} = 2.35 s (resonance condition). This case did not trigger the response in vertical direction since the two modes are not coupled.

With respect to the MSE loading case, as an example, Figure 4.8 and 4.9 shows the results for the displacement in Z direction and X direction, respectively, for the following three cases,

Case 1: T_g = 1.0 s and different T_d = 0.0 s, 0.5 s (i.e., 1/2 T_g), 1.2 s, 1.5 s

Case 2: T_g = 1.67 s and different T_d = 0.0 s, 0.5 s, 0.83 s (i.e., 1/2 T_g), 1.2 s, 1.5 s

Case 3: T_g = 2.0 s and different T_d = 0.5 s, 1.0 s (i.e., 1/2 T_g), 1.5 s

In the above three cases, the condition of T_d = 0.0 is used to represent the Uniform loading case. It can be seen in Fig. 4.8 (displacement for vertical direction) that Case 2 produces the largest displacement among the three cases. Such results are expected because, in Case 2, the period of the input ground motion reaches the nature period of the vertical mode of the frame, i.e. $T_g = T_{n2}$ = 1.66 s, which led to a resonance-like condition.

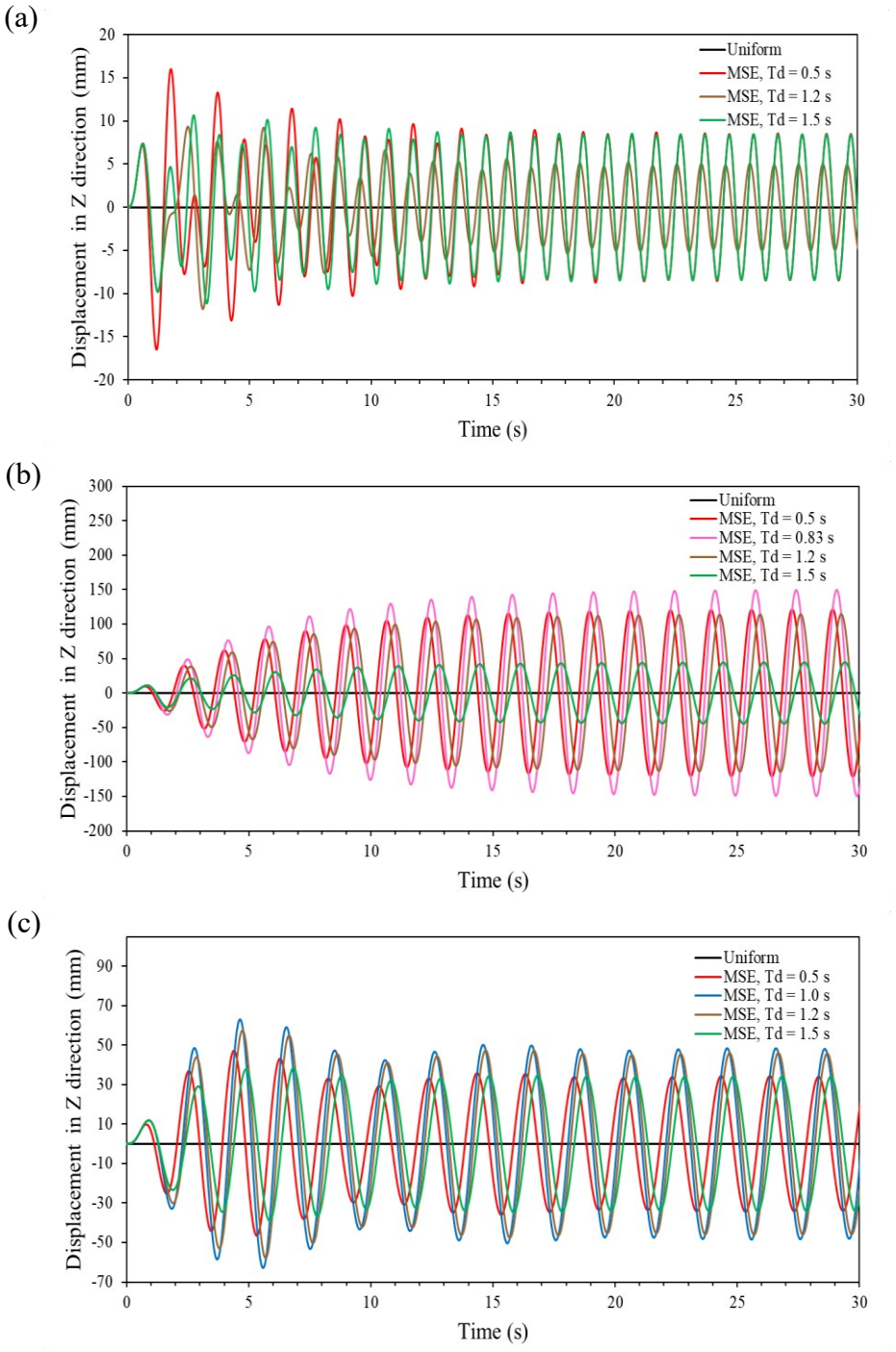

Figure 4.8 Vertical displacement from the 3 cases: (a) Case 1; (b) Case 2; (c) Case 3.

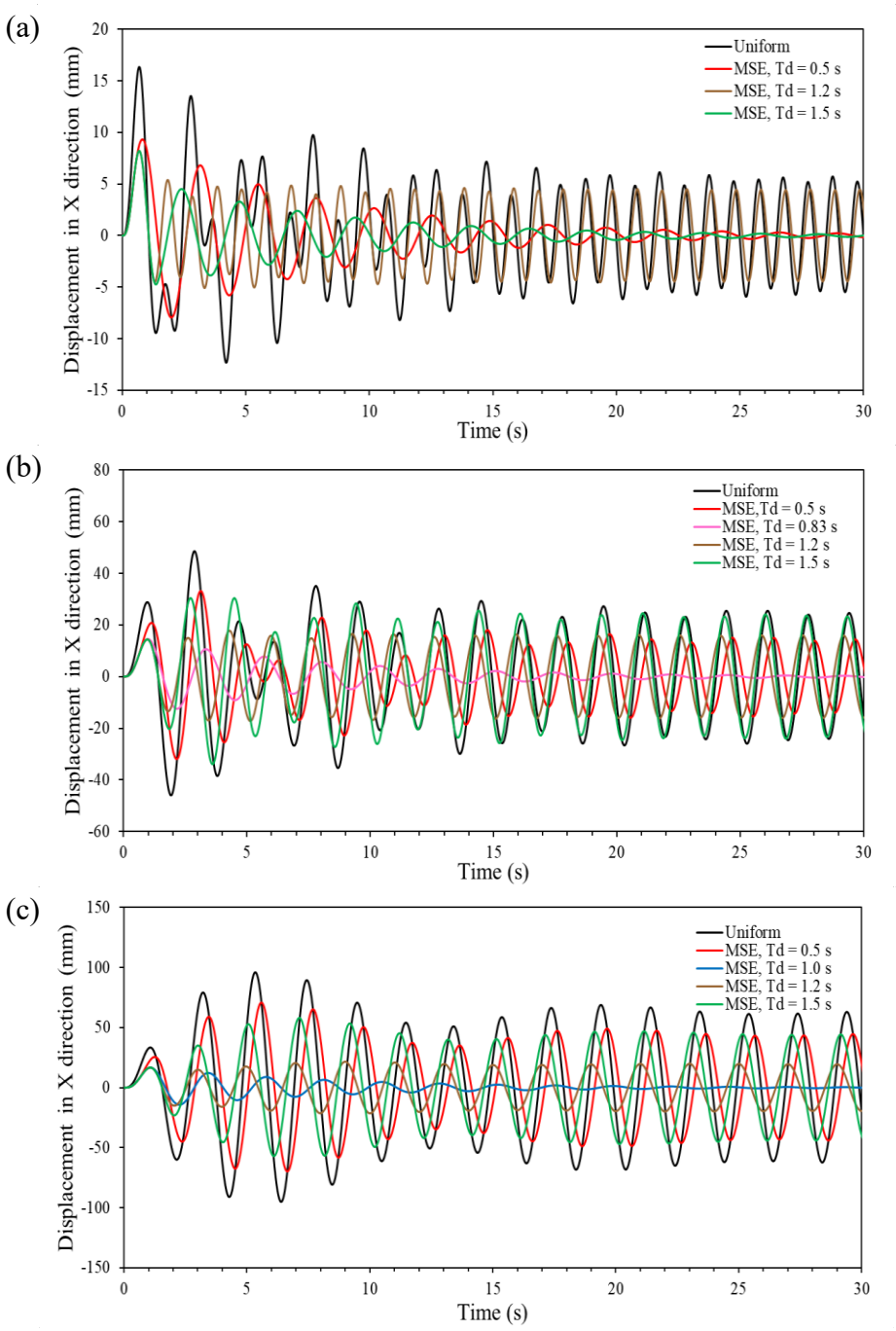

Figure 4.9 Horizontal displacement from the 3 cases: (a) Case 1; (b) Case 2; (c) Case 3.

It is necessary to mention that the term of resonance-like condition is introduced herein because the excitation applied and the response in question are not in the same direction. More specifically, the excitation is applied in the longitudinal direction while the response examined is in the vertical direction. However, for ease of discussion, the resonance-like condition is referred to as resonance hereafter in this thesis, in which the latter is typically referred to the condition where resonance is occurred in the direction of loading. Furthermore, resonance can be well identified in the steady-state response after 18s shown in Fig. 4.8b, in which the 5% damping affects the displacement and the displacement stays constant.

By comparing the response due to different delayed time presented in Fig. 4.8, it is noted that the maximum displacement is obtained when the delayed time equals to half of the period of the input motion ($T_d = 1/2T_g$), e.g., Case 1: $T_d = 0.5$ s; Case 2: $T_d = 0.83$ s; Case 3: $T_d = 1.0$ s.

The results in Fig. 4.8 clearly demonstrate that ***vertica***l response of the mass was obtained when the seismic excitation was assigned in the ***longitudinal*** direction and multi-support excitation was considered. Furthermore, the vertical resonance response is triggered in the above three cases mainly because of the fact that the two supports move against each other due to the time delayed, such as, $T_d = 1/2T_g$. More important, it is not related to the coupling effect since the two vibration modes of the frame examined are not coupled. Based on the observation of the results presented in Fig. 4.8, it can be concluded that a condition must be satisfied associated with the following three parameters, the

dominant period of the input ground motion, the natural period of the structure, and the delayed time considered in the excitation, in order to trigger the highest level of resonance. For the particular excitations examined for the system presented in Fig. 4.6, Equation 4.1 was proposed to formulate a condition where *the highest resonance level* for the response of the mass in vertical direction is generated due to seismic loading assigned in longitudinal direction and multi-support excitation is considered.

$$T_g = T_n \text{ and } T_d = ½\ T_g \tag{4.1}$$

Regarding the response in X direction (Fig. 4.9), the displacement from the Uniform loading case is larger than that from MSE loading case for the above mentioned three cases. This is consistent with the observation discussed in the section above. Therefore, no further analyses required.

4.4 Vertical resonance response due to MSE

4.4.1 Dominant period of the output response

The performance of a generic 2D frame system discussed in Section 4.3 indicates that vertical response would be triggered when a delayed time of the seismic wave is considered in the analysis. The highest level of this response (i.e. resonance) is achieved for the frame tested when the condition expressed in Eq. 4.1 is satisfied. Since the time delayed of the seismic excitation between the bridge supports depends on the velocity of the seismic wave. Given this, the analysis described in Section 4.2 was repeated for different velocities. The purpose of the analysis is to examine the condition among the follow three periods,

- T_g: period of the component of **Input** ground motion, which can also be referred to as frequency content of input ground motion since the period is the inverse of the frequency,
- T_n: natural period of the bridge, which can be also be represented by the dominant period of the **Output** or response, and
- T_d: delayed time of the seismic wave, which depends on the travelling distance and the wave velocity,

and to understand possible resonance of the vertical response of Bayview Bridge. The general procedure for the analysis is explained below, and it is also outlined in Fig. 4.10. A detailed VBA code of the analysis for this purpose prepared in this study is provided in Appendix A.

Step 1: Assign a value to velocity, and determine delayed time-histories to be assigned at the four supports of the bridge,

Step 2: Feed these time histories in SAP2000 model as an input ground motion for seismic analysis,

Step 3: Run analysis in SAP2000,

Step 4: Extract the maximum absolute displacement time-history at Joint 29,

Step 5: Repeat the analysis for other velocities.

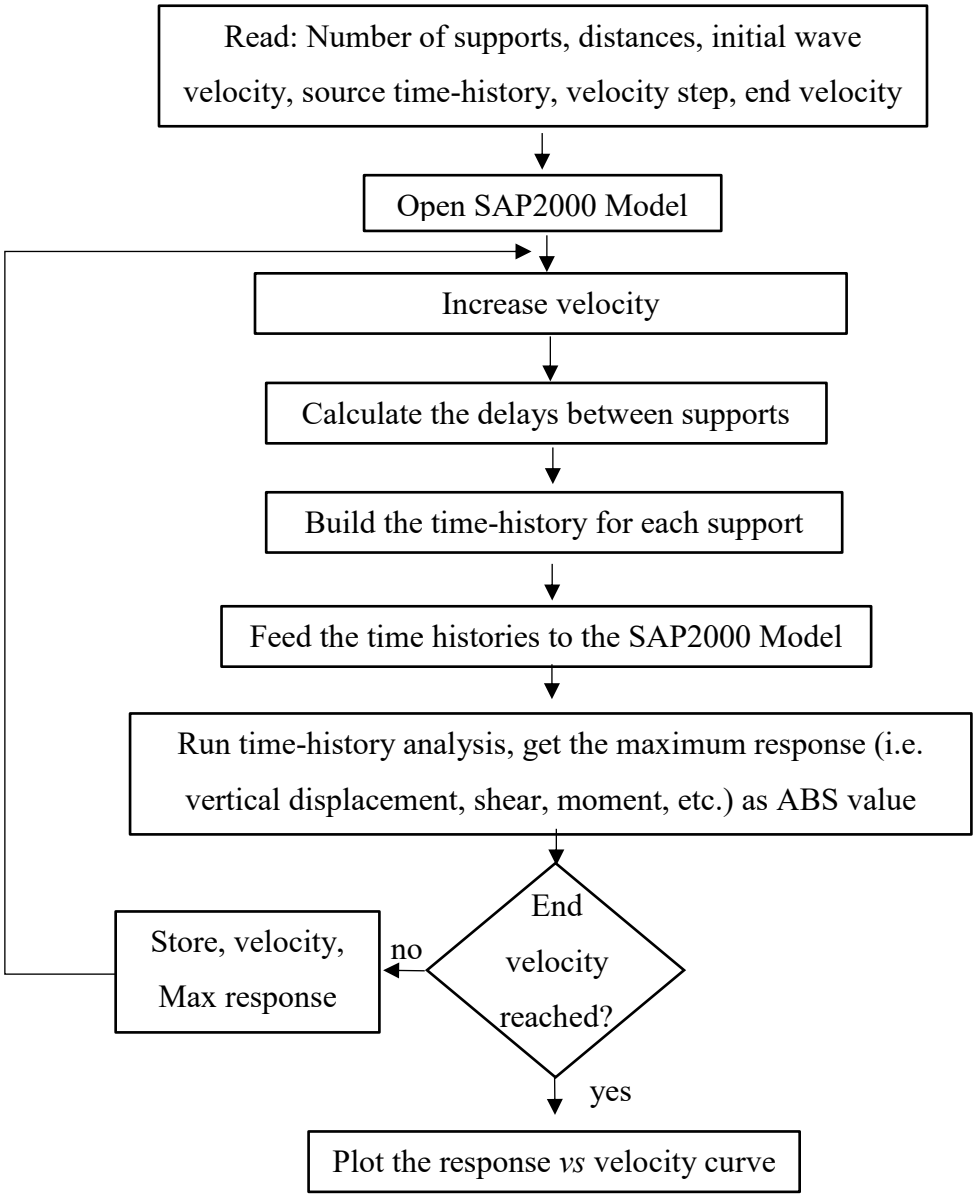

Figure 4.10 Flow chart for response *vs* velocity analysis.

Figure 4.11 presents the analysis results of the vertical displacement at joint 29 *vs* seismic wave velocity from the ten records. It is interesting to notice that, for all the records,

the peak of the displacement occurs at the velocity about 150 m/s except Re#4 whose peak occurs at the velocity of 90 m/s. It is not surprise that the displacement drops to zero at the velocity of about 3500 m/s, which can be considered as a Uniform loading case. This finding is consistent with the preliminary result discussed in Section 4.2, namely, no vertical displacement is generated from the Uniform loading case at Joint 29. The results in Fig. 4.11 also indicate that lower velocity is more critical for the vertical response than higher velocity as the delayed time is quite long.

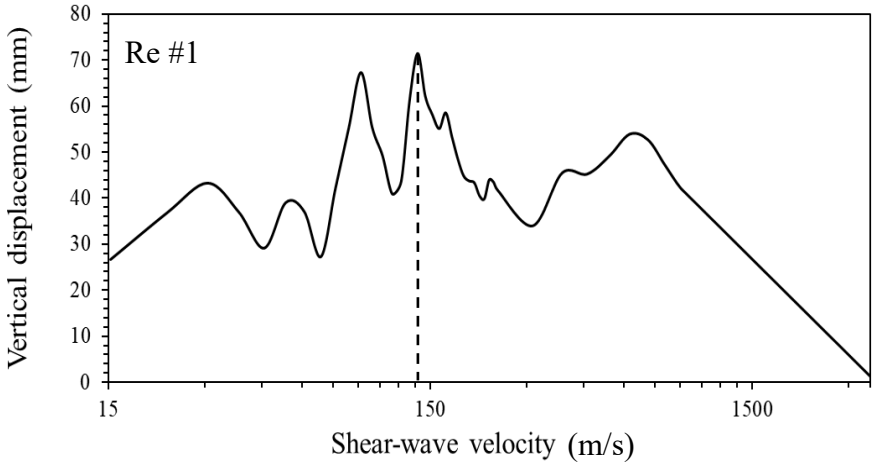

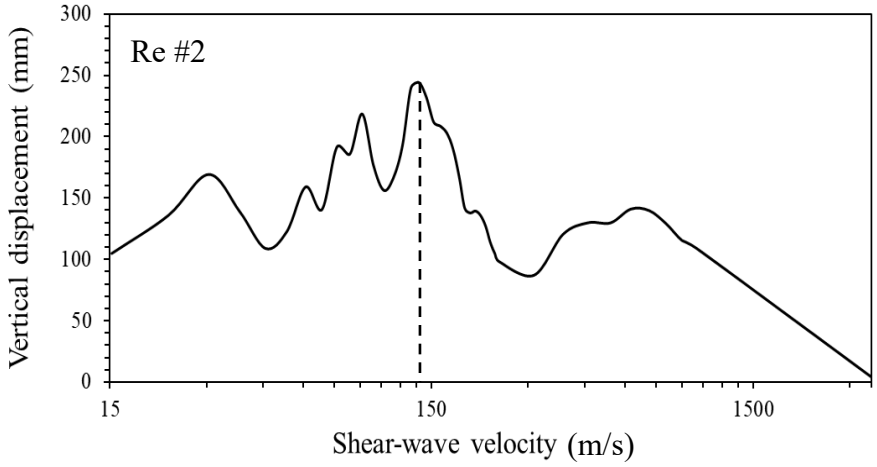

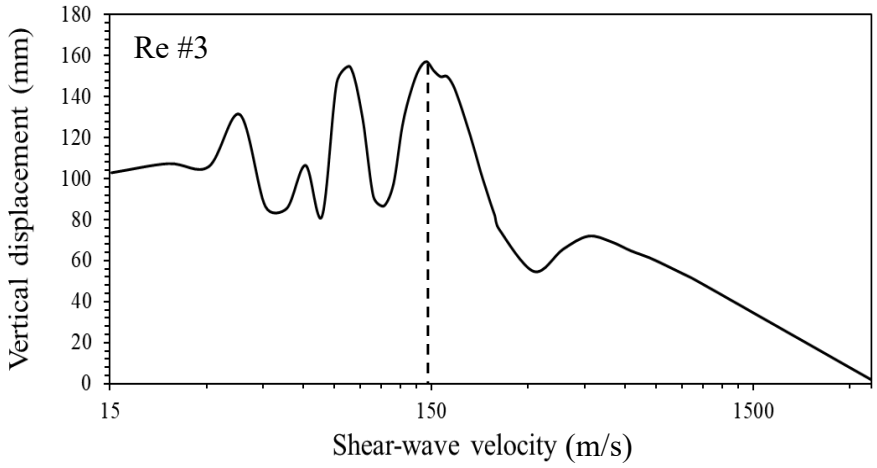
Re #3
Vertical displacement (mm)
180
160
140
120
100
80
60
40
20
0
15
150
1500
Shear-wave velocity (m/s)

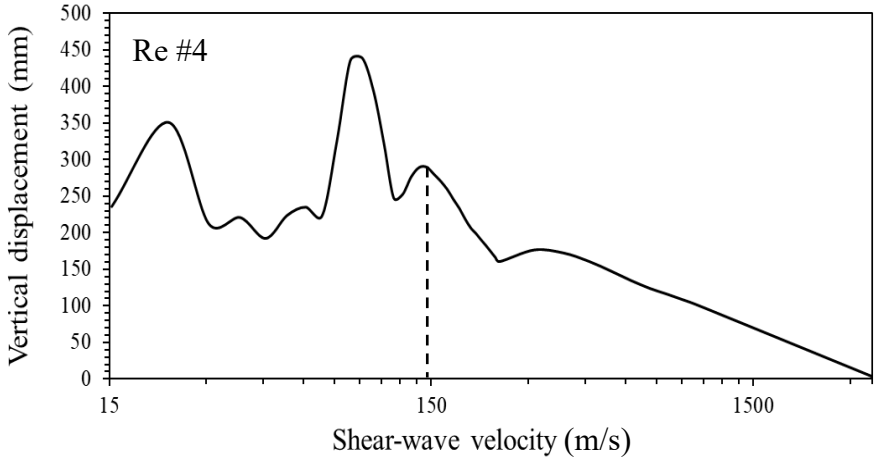
Re #4
Vertical displacement (mm)
500
450
400
350
300
250
200
150
100
50
0
15
150
1500
Shear-wave velocity (m/s)

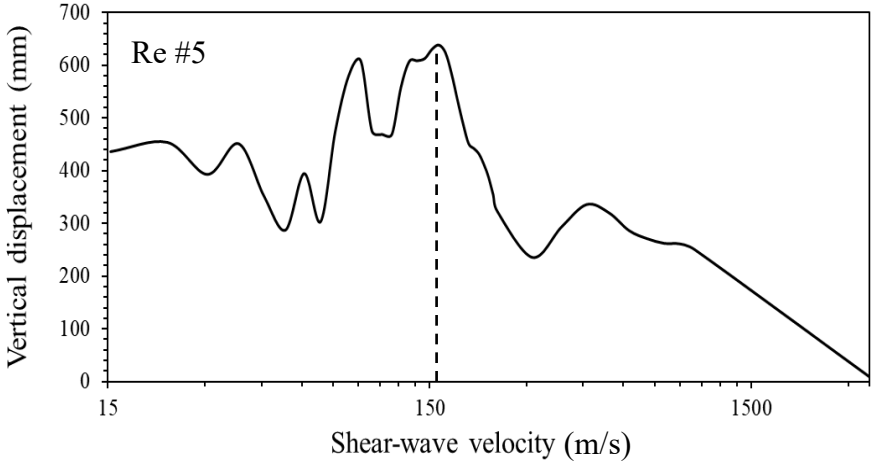
Re #5
Vertical displacement (mm)
700
600
500
400
300
200
100
0
15
150
1500
Shear-wave velocity (m/s)

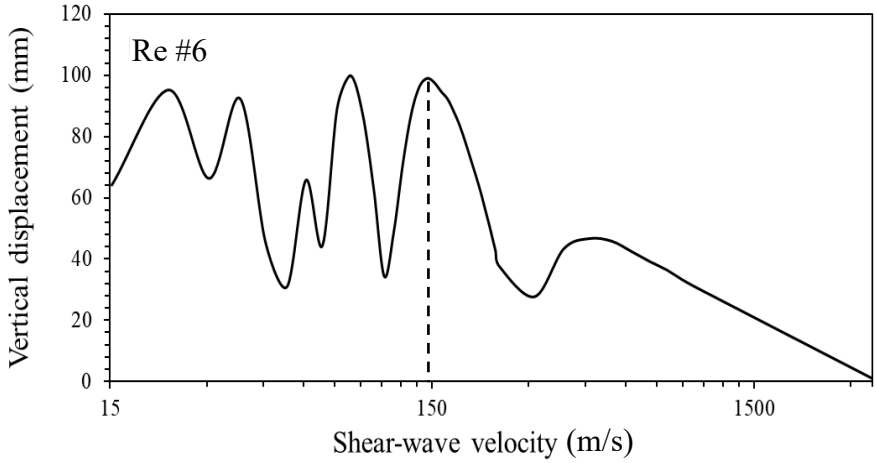
Re #6
Vertical displacement (mm)
120
100
80
60
40
20
0
15
150
1500
Shear-wave velocity (m/s)

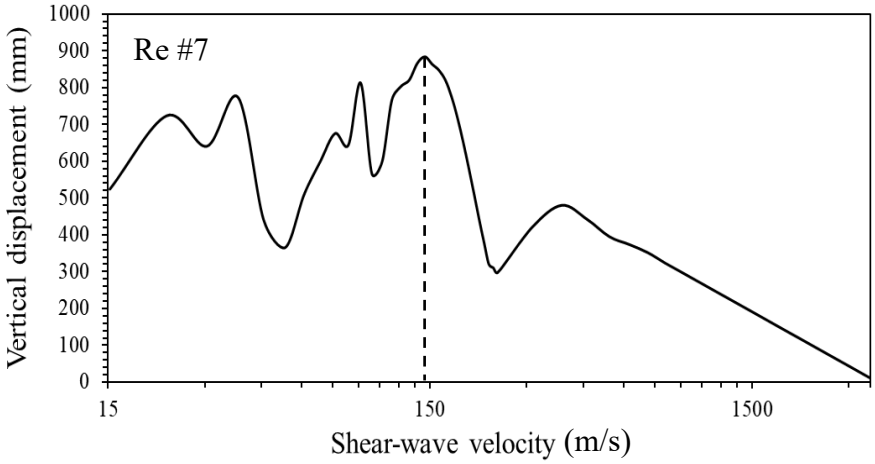
Re #7
Vertical displacement (mm)
1000
900
800
700
600
500
400
300
200
100
0
15
150
1500
Shear-wave velocity (m/s)

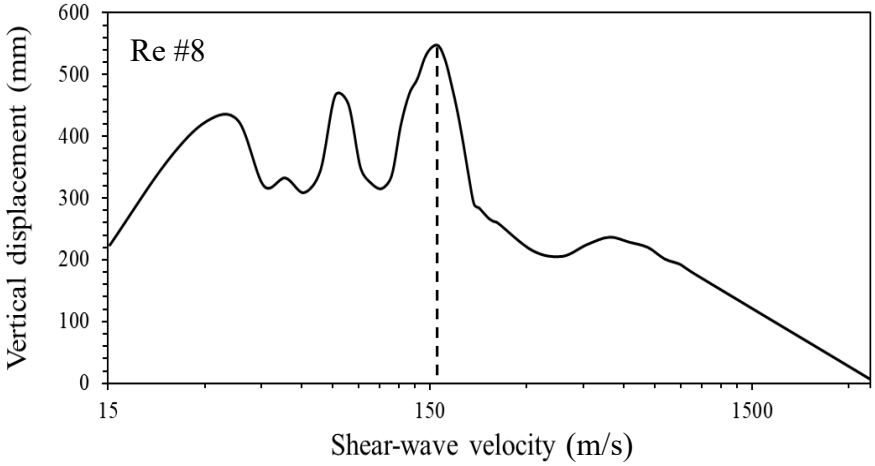
Re #8
Vertical displacement (mm)
600
500
400
300
200
100
0
15
150
1500
Shear-wave velocity (m/s)

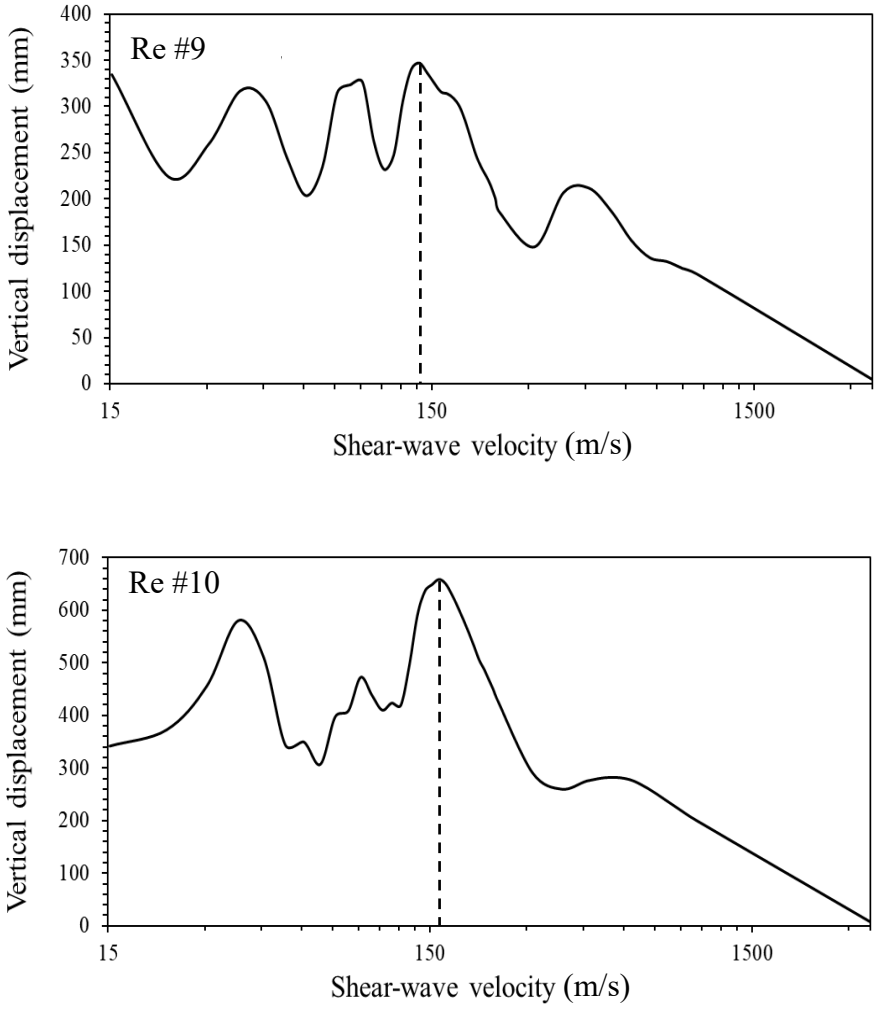

Figure 4.11 Displacement *vs* velocity curves.

To understand the bridge vertical response due to different velocities discussed above, Figure 4.12 was prepared for displacement spectra for joint 29 based on the results from MSE analysis using the delayed time due to velocity of 150 m/s and 90 m/s. It was found that the spectral displacement is dominant by the period of 2.67 s, which is equal to the natural period of the first vertical mode T_{n1} governing the vibration of Joint 29 in vertical direction (Table 3.2, Chapter 3). It should be noted that the system of Bayview Bridge is

quite complicated and multiple modes could contribute to dynamic response. Given this, it is not recommended to take the natural period of the first vertical mode from the modal analysis on the bridge model as the dominant period of the vertical response. In another word, it is better to determine the period that governs the response from displacement spectrum, i.e., spectral displacement vs mode period, as shown in Fig. 4.12.

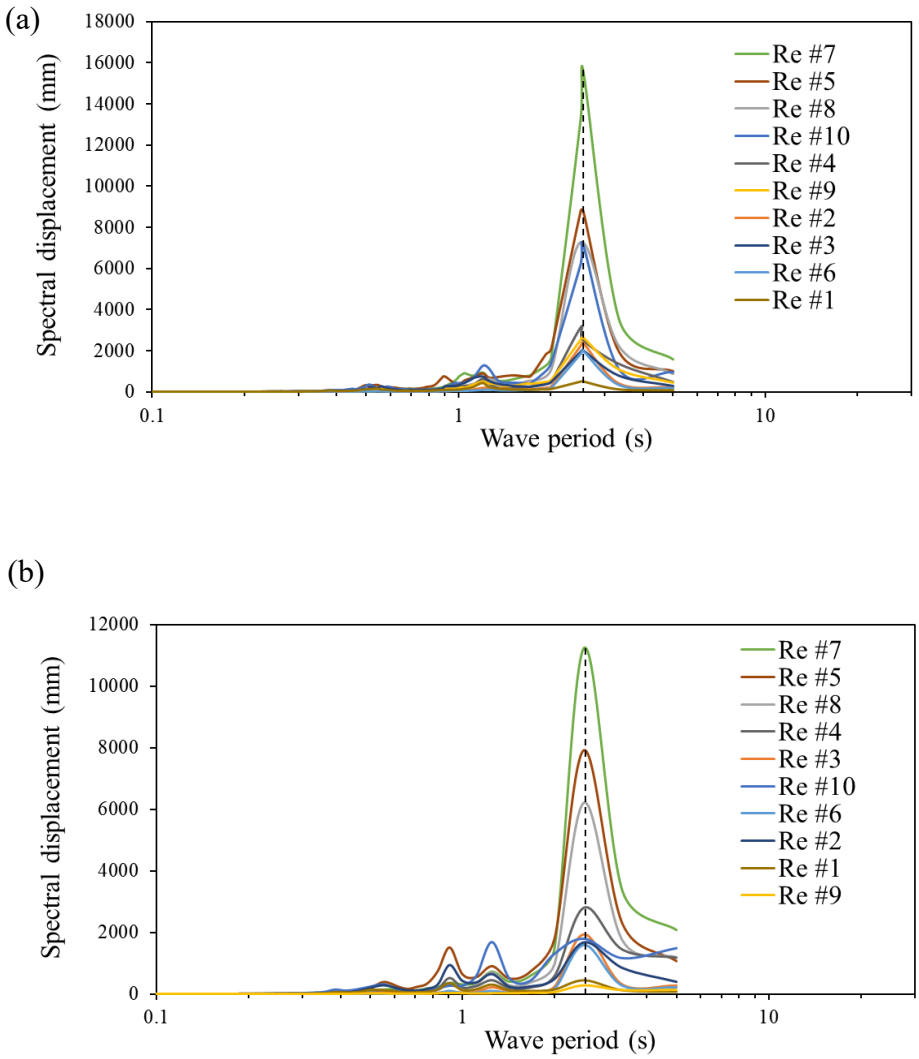

Figure 4.12 Displacement response spectra: (a) velocity = 150 m/s; (b) velocity = 90 m/s.

4.4.2 Frequency component of the input ground motion

To understand the frequency contents of the input ground motion, Fast Fourier Transform analysis was conducted on the displacement time-history of the ten records using software SeismoSignal and the results are presented in Fig. 4.13.

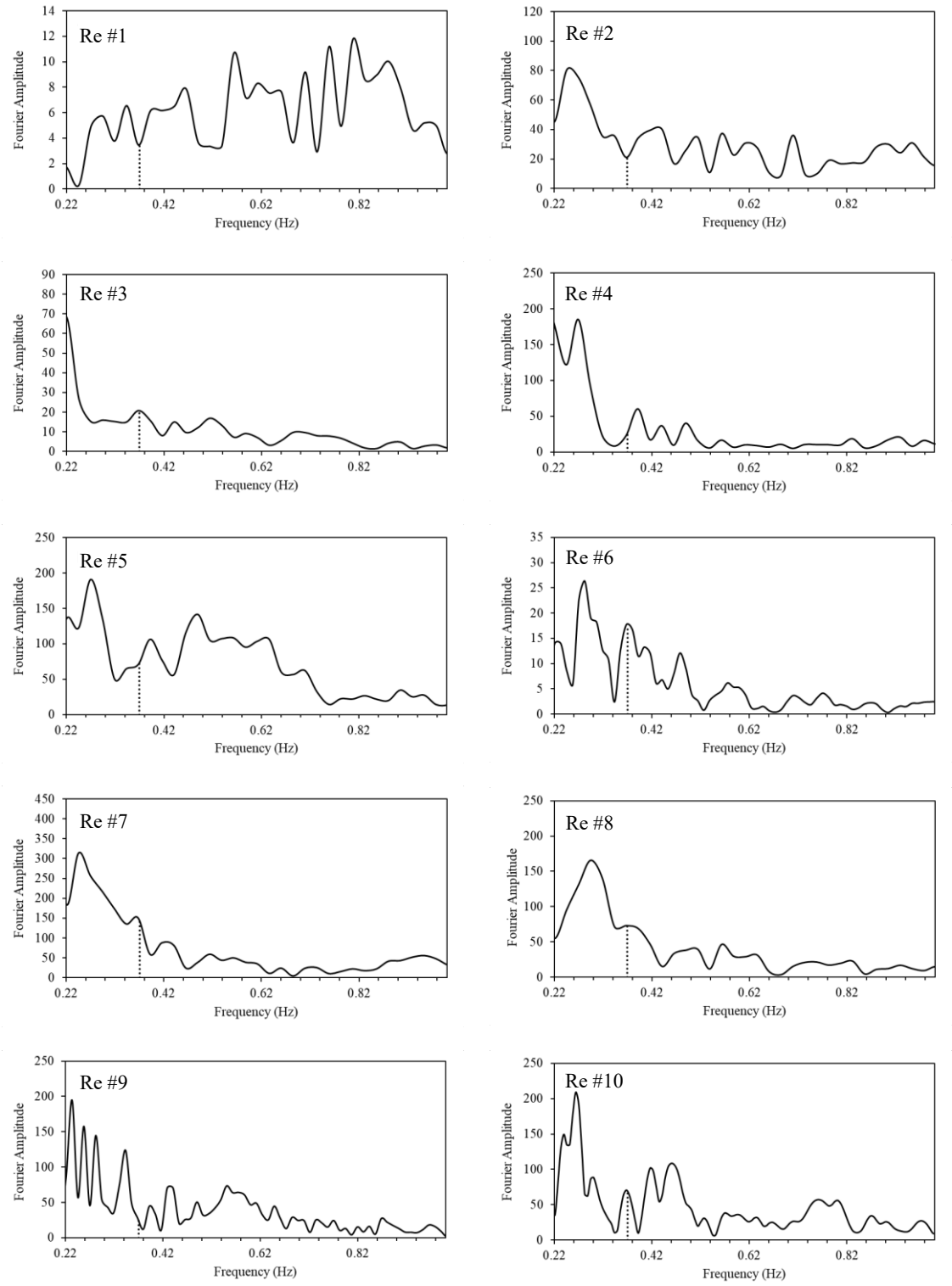

Figure 4.13 Fourier analysis results of each record.

The vertical dotted line in the figure is used to represent the frequency of the first vertical mode of Bayview Bridge of 0.37 Hz. Table 4.2 provides the Fourier amplitude of each record at the frequency of 0.37 Hz. For purpose of understanding the relation between spectral displacement and Fourier amplitude, the spectral displacement at the same frequency associated with seismic wave velocity of 150 m/s (Fig. 4.12a) for each record is also provided in Table 4.2.

Table 4.2 Fourier amplitude at dominate frequency of each record.

Record ID	Fourier amplitude @ 0.37 Hz (mm)	Spectral displacement at 150 m/s (mm)
Re #7	141.6	15700
Re #5	74.1	8850
Re #8	72.8	7300
Re #10	67.6	7190
Re #4	26.3	3170
Re #9	25.3	2640
Re #2	22.3	2400
Re #3	20.4	2020
Re #6	17.5	2020
Re #1	3.7	526

The results in Table 4.2 show that larger Fourier amplitude leads to larger spectral displacement. Furthermore, the results in Table 4.2 indicate relatively larger vertical displacement at Joint 29 was observed in Fig. 4.11 (e.g., 860 mm from Re #7; 640 mm from Re #5) is obtained because the frequency content of 0.37 Hz in the input ground motion was triggered and has led to resonance. As an example, Figure 4.14 illustrates the displacement time-history of Re #5 and Re #7 from MSE loading case and the delayed time was determined based on the wave velocity of 150 m/s. The shape of the time-history

confirms that the excitation of Re #5 and Re#7 generated resonance of the bridge vertical displacement.

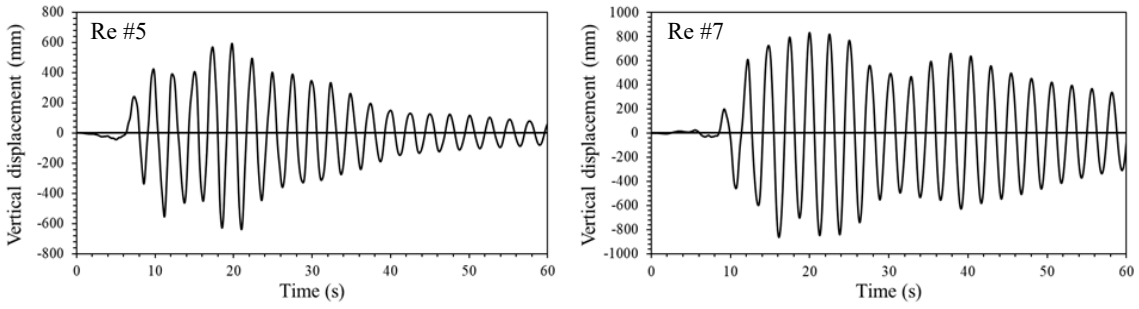

Figure 4.14 Displacement time-history for Joint 29: (a) Re #5; (b) Re #7.

Additional analysis was carried out in order to assess the effect of the frequency content of 0.37 Hz in the input ground motion on the response. Therefore, the displacement time-history of each record was processed to filter out the frequency content of 0.37 Hz. Then this new displacement time-history was used as an initial excitation and assigned at Support 1. The analysis described in Section 4.4.1 was then repeated and the results are presented in Fig. 4.15. It can be seen in Fig. 4.15 that the displacement is reduced significantly when the frequency of 0.37 Hz was removed from the input ground motion. The reduction factor of the response associated with each record w/o the frequency content of 0.37 Hz at the velocity of 150 m/s, which is the velocity corresponding to the peak displacement shown in Fig. 4.11, is listed in Table 4.3. It can be seen in the table that the response can be reduced as much as 5.9 times if the component of frequency of 0.37 Hz is filtered out. This indicates the frequency of 0.37 Hz has a significant contribution to the response. In addition, it is confirmed that the dominant frequency of 0.37 Hz (equivalent to T_g = 2.67 s) has led the resonance discussed above.

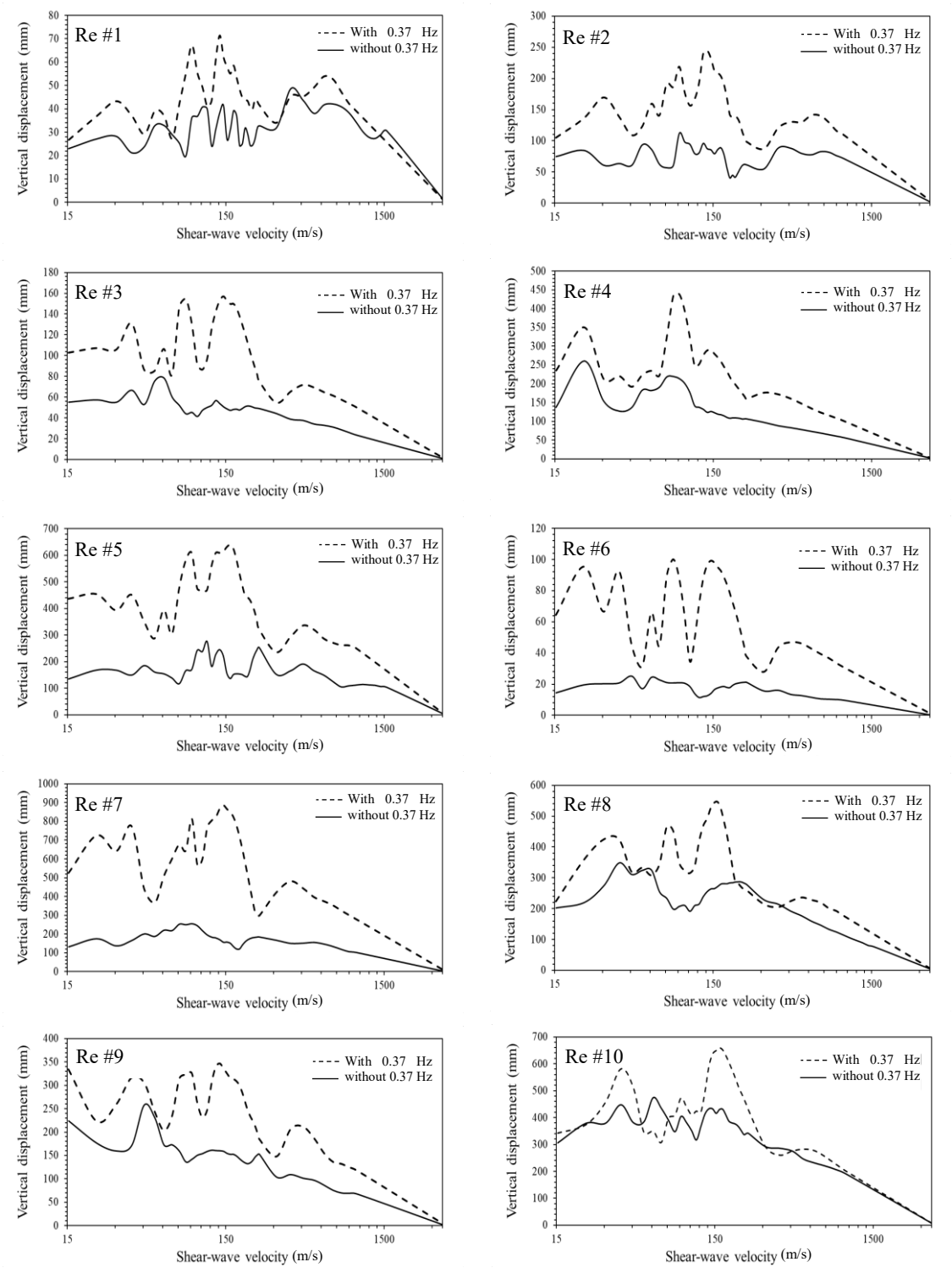

Figure 4.15 Displacement response w/o frequency content of 0.37 Hz.

Table 4.3 Displacement reduction ratio w/o 0.37 Hz.

Record ID	Displacement (mm)		Ratio
	without filtering 0.37 Hz	with filtering 0.37 Hz out	
Re #1	58	26	2.2
Re #2	212	79	2.6
Re #3	152	48	3.1
Re #4	280	122	2.2
Re #5	631	156	4.0
Re #6	98	16.5	5.9
Re #7	864	157	5.5
Re #8	544	268	2.0
Re #9	325	154	2.1
Re #10	648	415	1.5

4.4.3 Delay time

As discussed in Section 4.3, the cause of the vertical displacement of the mass in the frame illustrated in Fig. 4.6 is due to the delayed time when seismic wave travels from one support to another, which might make the two supports move against each other. Based on the above discussion, it can be concluded that the seismic wave velocity is critical in the seismic analysis using multi-support excitation. To determine the velocity that might trigger the highest level of resonance, a delayed time factor *D* is introduced in this study as expressed below,

$$D = \frac{T_g}{T_d} = \frac{T_n}{T_d} \tag{4.2}$$

$$T_d = \frac{Total\ bridge\ length}{seismic\ wave\ velocity\ leading\ to\ resonance} = \frac{L}{V_{s,r}} \tag{4.3}$$

From the above analysis results for Bayview Bridge, the following values are obtained,

L = 542 m, $V_{s,r}$ = 150 m/s, T_d = 3.61 s, $T_g = T_n$ = 2.67 s, D = 0.72

The benefit of introducing the two Equations 4.2 and 4.3 is, once the delay factor D is known, the velocity $V_{s,r}$ can be determined. Then this velocity can be compared with the shear-wave velocity provided by soil report to conclude if resonance would be a concern or not due to earthquake loads.

4.5 Determination of delayed time factor

This section is focused on investigation the delay factor on several generic cable-stayed bridges based on Bayview Bridge. In total, four bridges are examined and they are labelled as Tested Bridge #1, #2, #3, and #4. The analysis on the model of the four bridges follows the procedure outlined in Section 4.4 to obtain a curve for the vertical displacement at the middle of the second span *vs* seismic wave velocity for each record.

4.5.1 Tested Bridges #1 and #2

Tested Bridge #1 and Tested Bridge #2 were developed based on the model of Bayview Bridge. Tested Bridge #1 is softer than Bayview Bridge (i.e., it has a longer period compared to Bayview Bridge) while Tested Bridge #2 is stiffer than Bayview Bridge (i.e., it has a shorter period compared to Bayview Bridge). Below are the modifications made in the model of Bayview Bridge to derive a model for Tested Bridge #1 and Tested Bridge #2.

Tested Bridge #1:

- The stiffening wall between the legs of the pylon is removed,
- The vertical moment of inertia of the deck is reduced by 65%,
- The moment of inertia of pylons in the longitudinal direction is reduced by 50%, and all other parameters remain the same.

Tested Bridge #2:

- Only the vertical moment of inertia of the deck is increased four times, and all other parameters remain the same.

The results from the modal analysis on the two bridge models show that the period for the first vertical model T_n of the Tested Bridge #1 is 3.73 s, Tested Bridge #2 is 2.13 s. The results in Fig. 4.16 show that,

Tested Bridge #1, the resonance velocity $V_{s,r}$ = 105 m/s;

Tested Bridge #2, the resonance velocity, $V_{s,r}$ = 183 m/s.

By substituting $V_{s,r}$ into Eq. 4.3, the delayed time T_d

Tested Bridge #1, T_d = 5.16 s; Tested Bridge #2, T_d = 2.96 s

By substituting T_d and T_n into Eq. 4.2, the delayed time factor D

Tested Bridge #1, D = 3.73/5.16 = 0.722; Tested Bridge #2, D = 2.13/2.96 = 0.720.

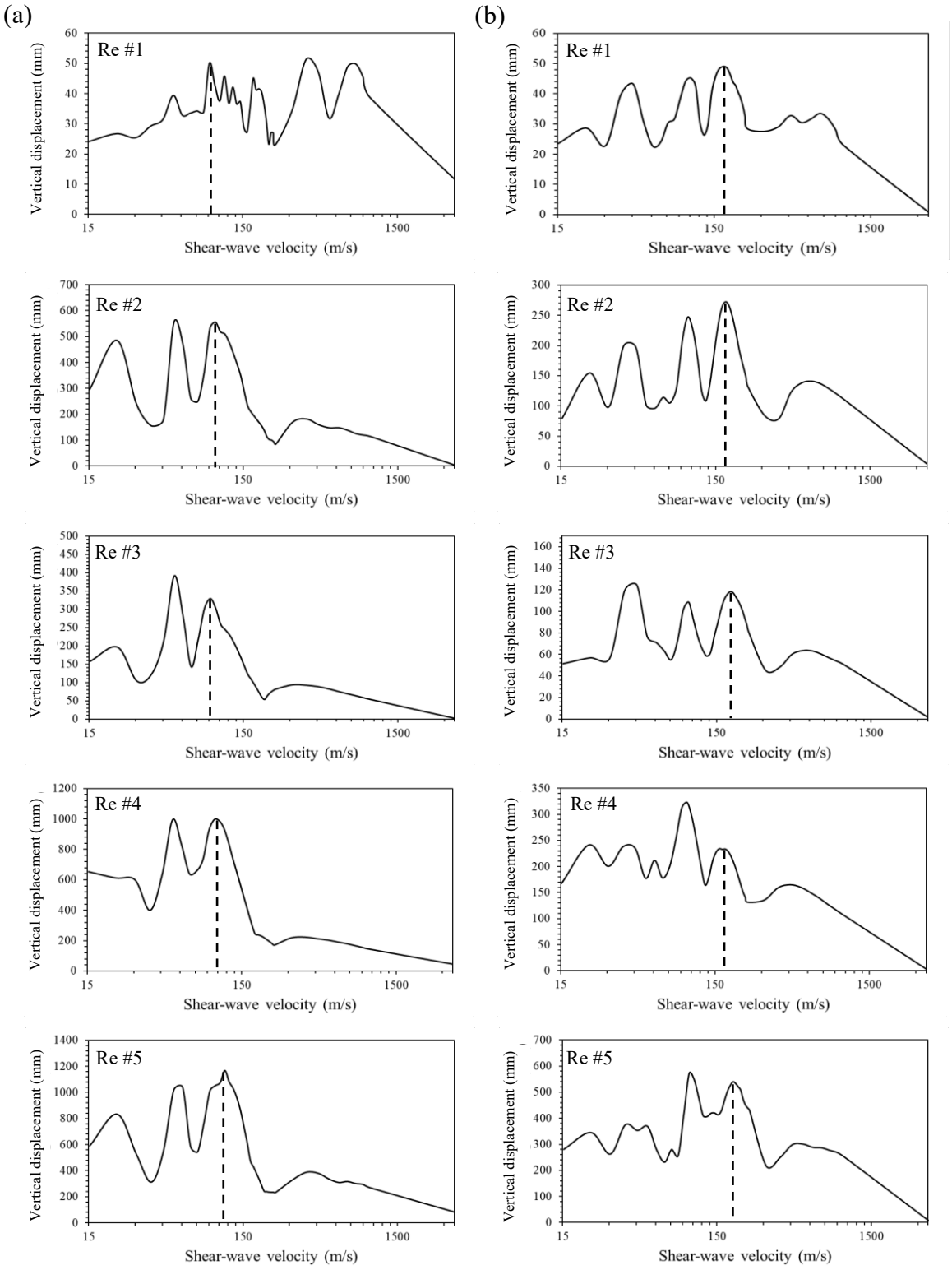
(a)
(b)
Re #1
Re #2
Re #3
Re #4
Re #5
Vertical displacement (mm)
Shear-wave velocity (m/s)
15
150
1500

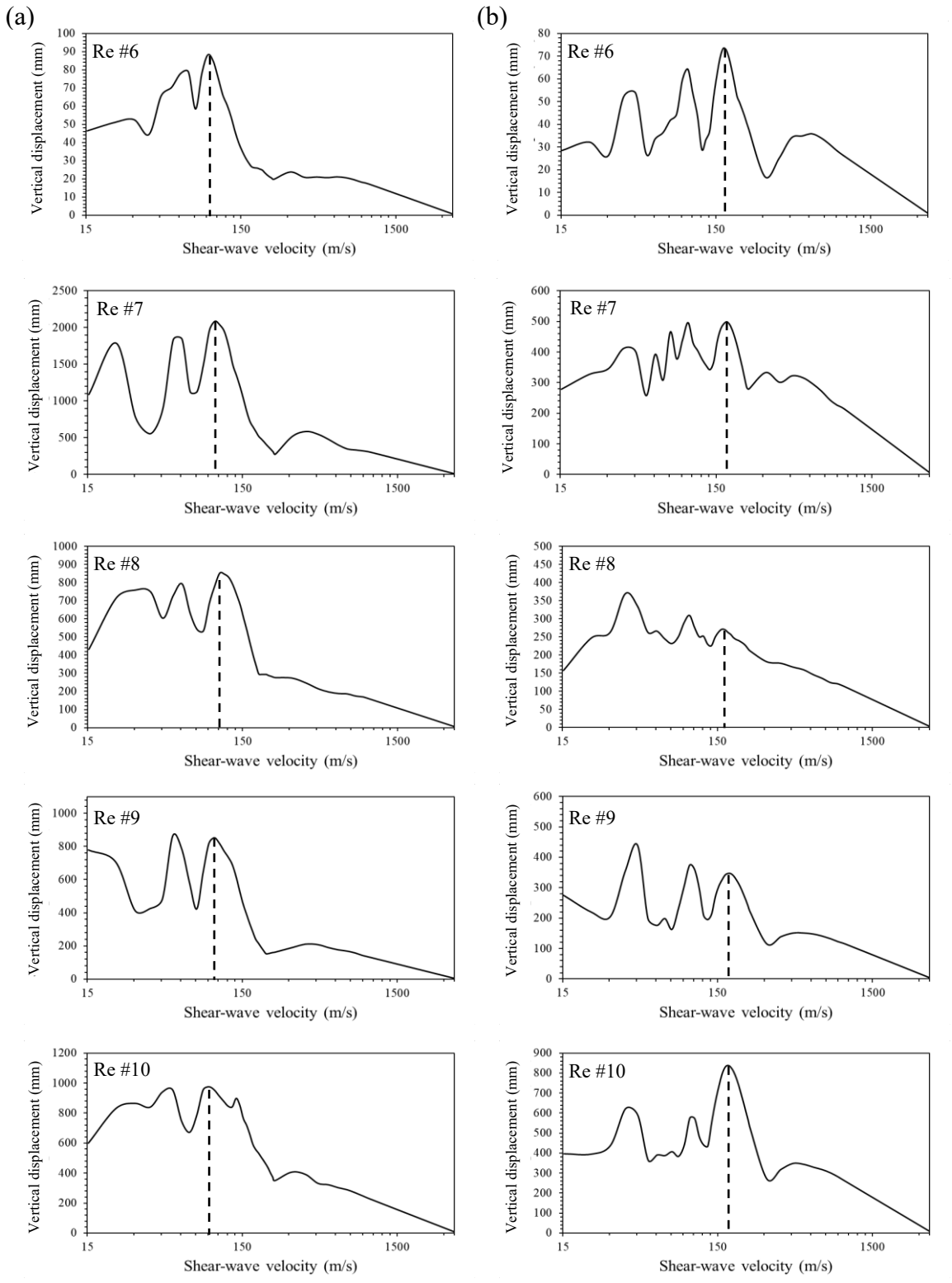

Figure 4.16 Displacement response for generic bridges: (a) Tested Bridge #1; (b) Tested Bridge #2.

4.5.2 Tested Bridges #3

Tested Bridge #3 (Fig. 4.17) was developed with modifications of the geometry of Bayview Bridge, namely, the span length of the tested bridge is 96 m+201m+96m with a total length of 393 m.

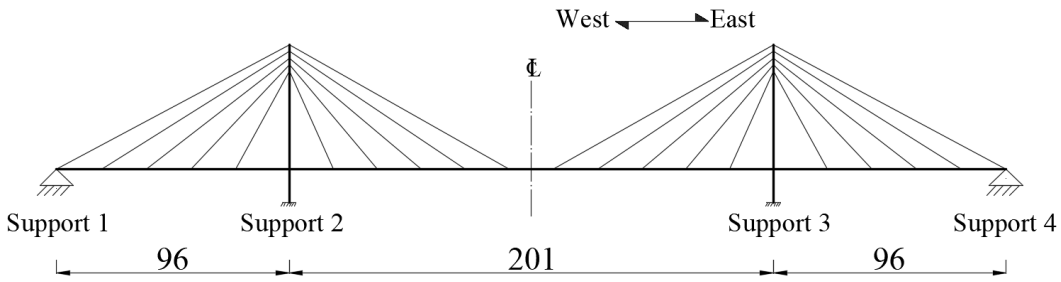

Figure 4.17 Elevation view of Tested Bridge #3.

The reasons for such choice are as follows,

- Keeping the ratio of the side span-to-main span of the bridge under the test (i.e., 0.477) closer to the Bayview Bridge (i.e., 0.485).
- It was reported by Gimsing and Georgakis (2012) that the optimum side-to-main span ratio for a commonly used 3-span cable-stayed bridge is about 0.38, which could be increased by 20-25% for conservatism (i.e., 0.456-0.475).
- It is not advisable to change the length of the segments in the model of the Bayview Bridge because any modification to the segment length will result in the change of the correction factors for the mass moment of inertia of the deck and some other modelling parameters. Therefore, the model of the

Tested Bridge #3 was developed by removing total eight segments from the superstructure of the Bayview Bridge, i.e., two from each of the side span and 4 from the main span while no change was made to all other input parameters.

The period of the first vertical mode T_n of the Tested Bridge #3 was found to be 1.815 s. The results of the displacement *vs* velocity (Fig. 4.18) show that the resonance velocity $V_{s,r}$ is about 156 m/s, which is almost the same as that for the Bayview Bridge. Using Equations 3 and 4, the delayed time factor D is taken as 0.720.

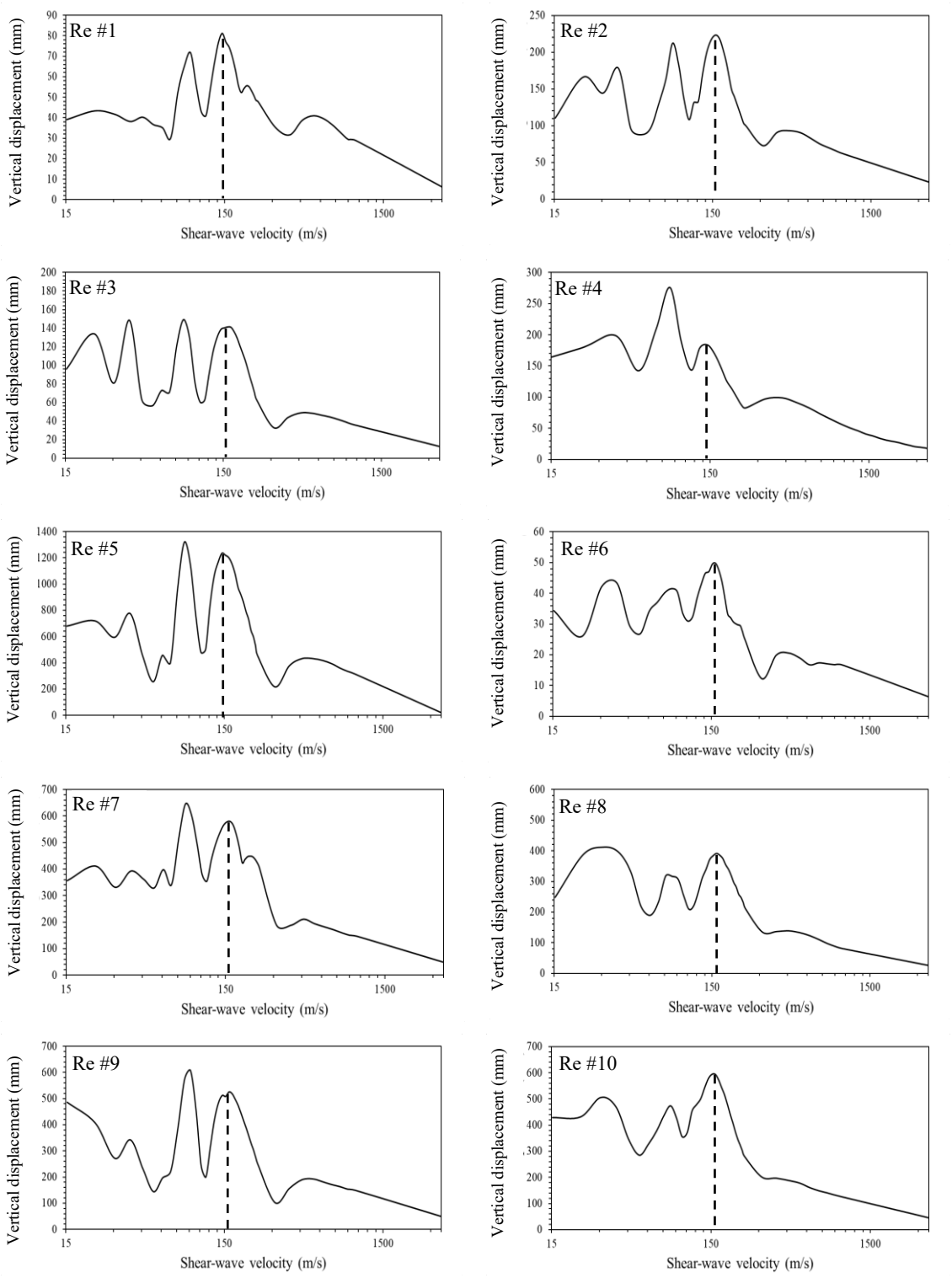

Figure 4.18 Displacement response for Tested Bridge #3.

4.5.3 Tested Bridge #4

The model of the Tested Bridge #4 was developed based on the model of the Tested Bridge #3, in which the axial stiffness of the cables was increased four times by applying a modification factor to cross sectional area of the cable as illustrated in Fig. 4.19. All other modeling parameters of Tested Bridge #4 are the same as those of Tested Bridge #3.

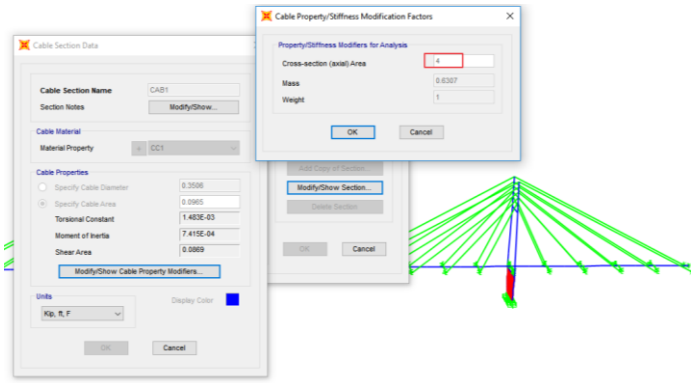

Figure 4.19 Input for axial stiffness in SAP2000.

The modal analysis on the model of the Tested Bridge #4 provides the period of the first vertical mode of the bridge T_n = 1.127 s. The results (Fig. 4.20) for the displacement *vs* seismic wave velocity show that the resonance velocity $V_{s,r}$ = 253 m/s. Using Eqs. 4.2 and 4.3, the delayed time factor D is equal to 0.727.

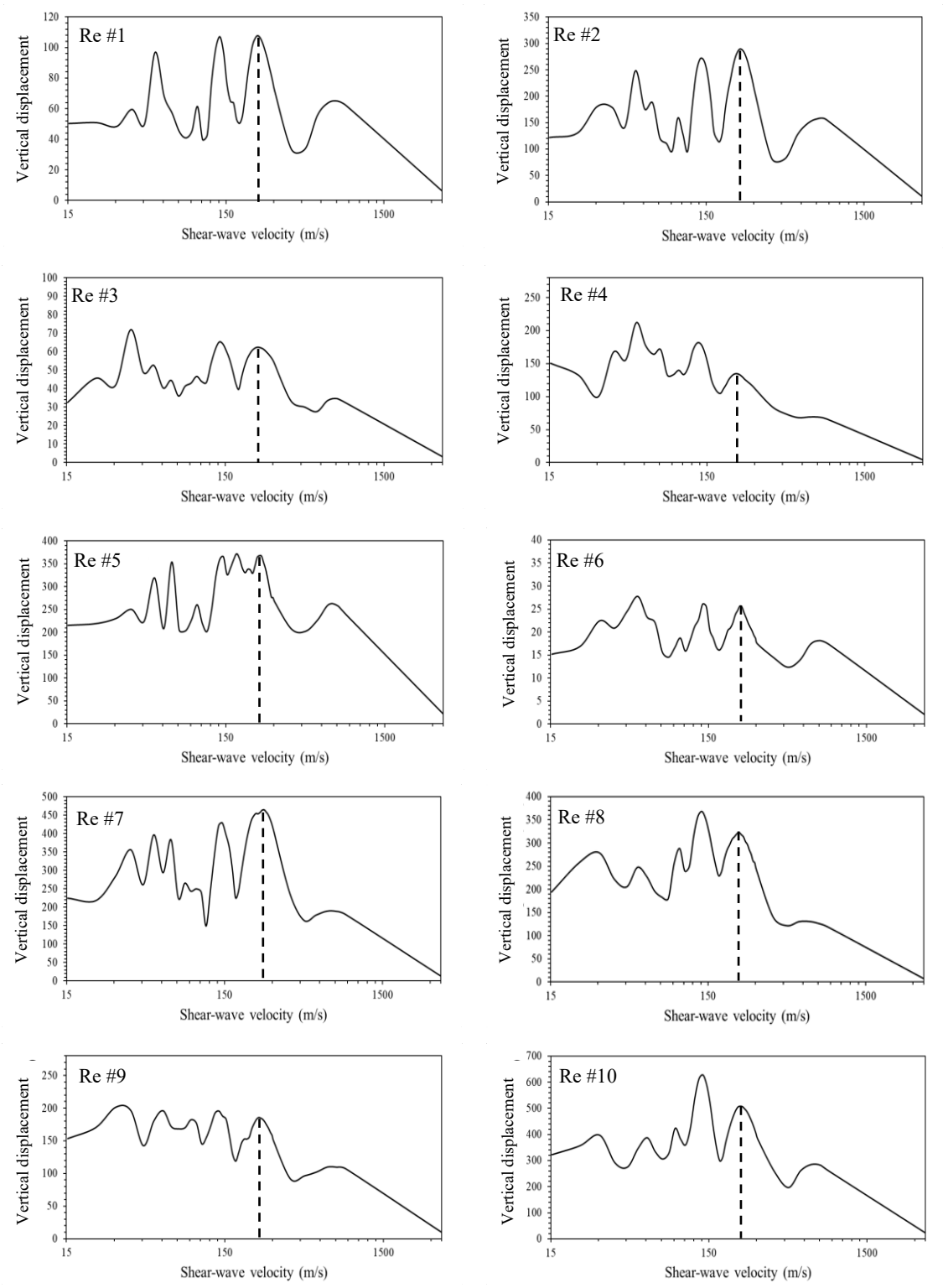

Figure 4.20 Displacement response for Tested Bridge #4.

4.5.4 Closing remarks

The analysis results of the four generic bridges under the examination show that the delayed time factors for Tested Bridges #1, #2, #3 and #4 are 0.722, 0.720, 0.720, and 0.727, respectively. For the Bayview Bridge, it is 0.720. Given this, a value of 0.72 is recommended as the delayed time factor. This factor can be used to determine the velocity that would cause the highest level of resonance to the vertical displacement at the middle of the main span of a typical 3-span cable-stayed bridge. This velocity can then be compared with the shear wave velocity of the soil on the bridge foundation in order to conclude if the resonance would be triggered for the safe design of the bridge.

Based on the results from this study, it can be reasonably assume that response much higher than the value of resonance might occur at a velocity less than the resonance velocity $V_{s,r}$. But this velocity normally might be relatively small which would be unrealistic in some cases though it has not been observed in this study.

Chapter 5

CONCLUSIONS

5.1 Introduction

The objective of this study is to evaluate the effects of spatial variation of seismic loads on the vertical response of typical 3-span cable-stayed bridges, and the potential of resonance due to different seismic wave velocity. For this purpose, Quincy Bayview Bridge located in Illinois, USA was selected for the study. The bridge was modelled using commercial software SAP2000 and was validated using the data from field test and previous studies. Linear time-history analysis was conducted using ten records obtained from severe earthquakes around the world.

A mathematical equation was developed to express the condition of resonance due to multi-support of excitation with phase delay. A time delay factor, which can be used to determine the wave velocity triggering the highest level of resonance on the bridge vertical displacement, was proposed. This factor was then tested on four generic 3-span cable-stayed bridges with a typical side to main span ratio of about 0.48.

5.2 Conclusions

The main conclusions drawn from this study are summarized as follows,

1. Multi-support excitation vs uniform excitation

    - The horizontal deck displacement from the uniform excitation is larger than that from the multi-support excitation. This observation is consistent with the finding from previous studies.
    - Significant vertical displacement is observed when the multi-support excitation is considered in the seismic analysis compared with the uniform excitation, in which the vertical displacement is zero for the latter.

2. Multi-support excitation

    - Attention is required for the bridge response in vertical direction under the horizontal seismic loading.
    - Lower seismic wave velocity (e.g., 200m/s vs 2000 m/s) tends to generate larger vertical displacement. Therefore, resonance might be triggered at low velocity.
    - Bridges seat on soft soil have a larger potential for resonance of vertical displacement compared with stiff soil. Alternatively, this resonance would not be an issue if the soil is classified as hard rock or very stiff soil.
    - Resonance of vertical displacement depends on the frequency content of the input ground motion, the dominant period of the vertical mode of the bridge, and the delayed time of the wave travelling from one support to another.

- For three-span cable-stayed bridges with a typical side to main span ratio of about 0.48, a factor of 0.72 is proposed to estimate the shear wave velocity that might trigger the vertical displacement in the resonance using the total length of the bridge.
- The mathematical equation proposed in Chapter 4 can be used to verify if resonance for a specific bridge would be possible.

5.3 Application

In practice, designers and researchers often do not pay attention to excessive vertical deck displacement of cable-stayed bridges subjected to earthquake loads. The results from this study will help to conclude if it might be a concern for commonly used three-span cable-stayed bridges with a typical side to main span ration of about 0.48. To reach a conclusion, following steps are recommended,

Step 1: Run modal analysis on the bridge model to obtain the period of the first vertical model T_n,

Step 2: Substitute delay factor D of 0.72 and T_n into Equation 4.2 to determine delay time T_d,

Step 3: Substitute T_d and the total length of the bridge L into Equation 4.3 to determine resonance velocity $V_{s,r}$,

Step 4: Compare $V_{s,r}$ with the shear velocity given in the geotechnical report. If they are relatively close, then responses in the vertical direction should be

checked carefully in the analysis. Otherwise, excessive vertical responses might not be a concern.

5.4 Limitations

This study focused on commonly used 3-span cable-stayed bridges with a typical side to main span ratio of about 0.48. Considering the complexity of cable-stayed bridges in terms of geometry, layout of cables, anchor system, etc., the conclusions from this study may not be valid for other bridges, e.g., 5-span bridges. However, the methodology established in the study can be followed to examine if resonance of the response in the vertical direction would become a concern.

The direction of the seismic loading considered in the study was the longitudinal direction, i.e., perpendicular to the bridge transverse direction. It is worth repeating the analysis outlined in this study to investigate the effect of the angle on the loading with respect to the transverse direction on the vertical response.

In this study, the towers are assumed fully fixed at the bottom. Therefore, soil-structure interaction was not considered in this study. Furthermore, given the scope of the research, the other two spatial effects (coherence effect and foundation effect), which have been reported to affect the multi-support excitation for seismic analysis of bridges, were not discussed in this thesis.

References

AASHTO. (2015). Guide Specifications for LRFD Seismic Bridge Design. American Association of State Highway and Transportation Officials.

Allam, S., and Datta, T. (2003). Seismic Response of Suspension Bridges Under Multi-Component Non-Stationary Random Ground Motion. Journal of Seismology and Earthquake Engineering, **5**(1): 15-29.

ASCE. (1992). Guidelines for Design of Cable-Stayed Bridges. American Society of Civil Engineers. doi:10.1061/9780872629004.

Aswathy, S., Kartha, U., and Mathai, A. (2013). Seismic Pounding of Bridges due to Multi-Support Excitation with traveling wave. American Journal of Engineering Research, **4**(RASE): 29-32.

ATC. (1996). Improved Seismic Design Criteria for California Bridges: Provisional Recommendations. Applied Technology Council. Available from https://books.google.ca/books?id=fEDmoQEACAAJ.

Berrah, M., and Kausel, E. (1993). A modal combination rule for spatially varying seismic motions. Earthquake Engineering and Structural Dynamics, **22**(9): 791-800.

CEN. (2004). Eurocode 8 - Design of Structures for Earthquake Resistance- Part 1: General Rules, Seismic Actions, and Rules for Buildings. European Standard Norme.

CEN. (2005). Eurocode 8 - Design of Structures for Earthquake Resistance - Part 2: Bridges. European Standard Norme.

Chopra, A. (2011). Dynamics of Structures Theory and Applications to Earthquake Engineering. 4th Edition. Berkeley, CA: Pearson.

Christian, J. (1976). Relative motion of two points during an earthquake. Journal of Geotechnical and Geoinveronmental Engineering, **102**(11): 1191-1194.

Crewe, A., and Norman, J. (2006). Experimental Modelling of Multiple Support Excitation of Long Span Bridges. Proceedings of the 4th International Conference on Earthquake Engineering. Taipei, Taiwan.

CSA-S6-14. (2014). Canadian Highway Bridge Design Code (CHBDC). Canadian Standard Association, Ottawa, Ont.

Ernst, H. (1965). Der E-Modul von Seilen unter Beriicksiehtigung. Der Buuingenieur, **40**(2): 52-55.

Fleming. (1978). Nonlinear Static Analysis of Cable-Stayed Bridge Structures. Computer and Structures, **10**(4): 621-635.

Fleming, J., Zenk, J., and Fabian, R. (1983). Nonlinear Behavior of Cable Stayed Bridges. Civil Engineering for Practicing and Design Engineers, **2**(3): 325-343.

Gimsing, N., and Georgakis, C. (2012). Cable Supported Bridges: Concept and Design. Chichester, United Kingdom: John Wiley and Sons, LTD.

Gong, Y., Park, M.Y., Choi, S.H., Kim, S., and Cheung, H.J. (2015). Multi-support excitation test of single-pylon cable-stayed bridge using shaking table. Journal of the Earthquake Engineering Society of Korea, **19**(4):161-171.

Harichandran, R., and Vanmarcke, E. (1986). Stochastic Vartion of Earthquake Ground Motion in Space and Time. Jourmal of Engineering Mechanics, **112**(2): 154-174.

Heredia-Zavoni, E., and Vanmarcke, E. (1994). Seismic Random-Vibration Analysis of Multisupport-Structural Systems. Journal of Engineering Mechanics, **120**(5): 1107-1128.

Hua, C.H., and Wang, Y.C. (1996). Three-Dimensional Modelling of a Cable-Stayed Bridge for Dynamic Analysis. Proceedings of the 14th International Modal Analysis Conference, Taiwan, pp. 1565-1571.

Jangid, R. (2013). Introduction to Earthquake Engineering. Available from http://nptel.ac.in/courses/105101004/ [cited 20 May 2018].

Japan Road Association. (2012). Japanese Design Specifications for Highway Bridges.

Kiuregihan, A., and Neuenhofer. (1992). Response Spectrum Method for Multi-Support Seismic excitations. Earthquake Engineering and Structural Dynamics, **21**(8): 713-740.

Leonhardt, F., and Zellner,, W. (1980). Cable-Stayed Bridges: Report on Latest Developments. Proceedings of the Canadian Structural Engineering Conference, Toronto, pp. 21-48.

Li, J., and Li, J. (2004). An Efficient Response Spectrum Analysis of Structures Under Multi-Support Seismic Excitations. Proceedings of the **13**th World Conference on Earthquake Engineering, Vancouver.

Loh, C.H., and Yeh, Y.T. (1988). Spatial Variation and Stochastic Modelling of Seismic Differential Ground Motion. Earthquake Engineering and Structural Dynamics, **16**(4): 583-596.

Nazmy, A., and Abdel-Ghaffar, A. (1990). Non-Linear Earthquake Response Analysis of Long-Span Cable-Stayed Bridges: Applications. Earthquake engineering and structural dynamics, **19**(1): 63-76.

Nazmy, A., and Abdel-Ghaffar, A. (1990). Three-Dimensional Nonlinear Static Analysis of Cable-Stayed Bridges. Computers and Structures, **34**(2): 257-271.

O'Rourke, M. J., Bloom, M., and Dobry, R. (1982). Apparent Propagation Velocity of Body Waves. Earthquake Engineering and Structural Dynamics, **10**(2): 283-294.

Poddar, K., and Rahman, T. (2015). Comparative Study of Cable Stayed, Suspension and Composite Bridge. International Journal of Innovative Research in Science, Engineering and Technology, **4**(9): 8530-8540.

Pridham , B., and Wilson, J. (2005). A Reassessment of Dynamic Characteristics of the Quincy Bayview Bridge Using Output-Only Identification Techniques. Earthquake Engineering and Structural Dynamics, **34**(7): 787-805.

Sextos, A., and Kappos, A. (2005). Evaluation of the New Eurocode8-Part 2 Provisions Regarding Asynchronous Excitation of Irrigular Bridges. Proceedings of the 4th European Workshop on the Seismic Behaviour of Irrigular and Complex Structures, Thessaloniki, pp. 26-27.

Sextos, A., Pitilakis, K., and Kappos, A. (2003). Inelastic Dynamic Analysis of RC Bridges Accounting For Spatial Variability of Ground Motion, Site Effects and Soil-Structure Interaction Phenomena Part 1: Methodology and Analytical Tools. Earthquake Engineering and Structural Dynamics, **32**(4): 607-627.

Tian, Z.Y., and Lou, M.L. (2014). Traveling Wave Resonance and Simplified Analysis Method for Long-Span Symmetrical Cable-Stayed Bridges under Seismic Traveling Wave Excitation. Shock and Viberation. Available from http://dx.doi.org/10.1155/2014/602825.

Tung, D., and Kudder, R. (1968). Analysis of Cables as Equivalent Two-Force Members. Engineering Journal American Institute of Steel Construction, **5**(1): 12-19.

Wilson, E. (2004). Static and Dynamic Analysis of Structures. 4th edition. Berkeley, CA: Computers and Structures, Inc.

Wilson, J., and Gravelle, W. (1991). Modelling of a Cable-Stayed Bridge for Dynamic Analysis. Earthquake Engineering and Structural Dynamics, **20**(8): 707-721.

Wilson, J., and Liu, T. (1991). Ambient Vibration Measurments on a Cable-Stayed Bridge. Earthquake Engineering and Structural Dynamics, **20**(8): 723-747.

Yang, C.Y., Cheung, M., and Xu, X. (2012). Wave Propagation Effect on Seismic Response of Cable-stayed Bridge: A Multiple Shake Tables Test. Proceedings of the **15**th World Conference on Earthquake Engineering. Lisbon.

Zadeh, O. (2012). Comparison Between Three Types of Cable Stayed Bridges Using Structural Optimization. M. A. Sc thesis, Department of Civil and Environmental Engineering, University of Western Ontario. London. Ontario.

Zerva, A. (1991). Effect of Spatial Variability and Propagation of Seismic Ground Motions on the Response of Multiply Supported Structures. In Stochastic Structural Dynamics 2. Springer. pp. 307-336.

APPENDIX A

RESPONSE *VS* VELOCITY CURVE CODE

```
Private Sub CommandButton1_Click()
'dimension variables
      Dim SapObject As cOAPI
      Dim SapModel As cSapModel
      Dim FileName As String
      Dim ret As Long
      Dim q1 As Variant, q2 As Variant
      Dim i As Integer, n As Integer
      Dim t() As Single, Tini As Single
      Dim THsource() As Single, TH() As Single
      Dim Tstart As Single, Tend As Single, Deltat As Single,
Vstart As Single
      Dim td As Single, count As Integer, points As Integer
      Dim inc As Single, Trials As Integer, j As Variant, V() As
Single
     Dim Result() As Double, ResultX() As Double
     Dim w As Variant
     Dim Dis() As Single
' Reading Data (velocity increasemet, end time, Delta t, indicial
velocity, number of trials, and ground motion record number)
inc = Val(txt1.Text): Tend = Val(txt2.Text): Deltat =
Val(txt3.Text): Vstart = txt7.Text
Trials = Val(txt4.Text): points = Val(txt6.Text)
n = Round(Tend / Deltat)
ReDim t(0 To n), TH(0 To 4, 0 To n), Dis(2 To 4), V(0 To Trials)
ReDim Result(0 To Trials), ResultX(0 To Trials)
ReDim THsource(0 To points)
Dis(2) = 440: Dis(3) = 1340: Dis(4) = 1780:
```

```
'Load the TH
q1 = "C:\Users\Bashar\Desktop\Thesis\BackUp Programs\THsource.txt"
Open q1 For Input As #1
  For i = 0 To points
      Input #1, x$: THsource(i) = x$
  Next i
Close #1
td = points * Deltat
   'create Sap2000 object
    Set SapObject = CreateObject("CSI.SAP2000.API.SapObject")
   'start Sap2000 application
   SapObject.ApplicationStart

   'create SapModel object
     Set SapModel = SapObject.SapModel

   'initialize model
     ret = SapModel.InitializeNewModel

   'open an existing file
    FileName                                                    =
"C:\Users\Bashar\Desktop\Thesis\Model\26_12_2017.sdb"
    ret = SapModel.File.OpenFile(FileName)



'Change the TH for each support
For w = 0 To Trials
    If w <> 0 Then V(w) = Vstart + inc * (w - 1)
  For j = 2 To 4

   If w <> 0 Then Tstart = Dis(j) / V(w)
If w = 0 Then Tstart = 0
count = 0
  For i = 0 To n
```

```
      t(i) = i * Deltat
      If t(i) < Tstart Then TH(j, i) = 0: count = count + 1
      If t(i) >= Tstart And t(i) < (td + Tstart) Then
      TH(j, i) = THsource(i - count)
      End If
      If t(i) >= (td + Tstart) Then TH(j, i) =
THsource(UBound(THsource()))
   Next i
'Save the THs
q2 = "C:\Users\Bashar\Desktop\Thesis\BackUp Programs\TH" & j &
".txt"
Open q2 For Output As #1
  For i = 0 To n
      Print #1, TH(j, i)
  Next i
Close #1
   Next j
'Run the Analysis
 ret                                                    =
SapModel.File.Save("C:\Users\Bashar\Desktop\Thesis\Model\26_12_20
17.sdb")
 ret = SapModel.Analyze.RunAnalysis
'Get the Results (SAP2000 objects)
Dim NumberResults As Long
      Dim Obj() As String
      Dim Elm() As String
      Dim LoadCase() As String
      Dim StepType() As String
      Dim StepNum() As Double
      Dim U1() As Double
      Dim U2() As Double
      Dim U3() As Double
      Dim R1() As Double
      Dim R2() As Double
      Dim R3() As Double
```

```
      Dim DType() As String
      Dim Value() As Double
      Dim SF() As Double
      Dim GD() As String
      Dim SapResult(6) As Double
   'clear all case and combo output selections
      ret                                                    =
SapModel.Results.Setup.DeselectAllCasesAndCombosForOutput


   'set case and combo output selections
      ret                                                    =
SapModel.Results.Setup.SetCaseSelectedForOutput("TH_EL_SAME_180_U
1")
      ret = SapModel.Results.JointDispl("100030", GroupElm, "2",
Obj, Elm, LoadCase, StepType, StepNum, U1, U2, U3, R1, R2, R3)
      ret      =      SapModel.Results.GeneralizedDispl("GDISP1",
NumberResults, GD, LoadCase, StepType, StepNum, DType, Value)


     SapResult(1) = U3(0)
     SapResult(2) = U3(1)
     SapResult(3) = Value(0)
     SapResult(4) = Value(1)
             If Abs(SapResult(1)) >= Abs(SapResult(2)) Then
                 Result(w) = Abs(SapResult(1))
              Else
                 Result(w) = Abs(SapResult(2))
             End If
            If Abs(SapResult(3)) >= Abs(SapResult(4)) Then
                ResultX(w) = Abs(SapResult(3))
             Else
                ResultX(w) = Abs(SapResult(4))
            End If
```

```
Cells(w + 1, 1) = V(w)
Cells(w + 1, 2) = Result(w)
Cells(w + 1, 3) = ResultX(w)
    ret = SapModel.Analyze.DeleteResults("Modal")

Next w
 'close Sap2000
      SapObject.ApplicationExit False
      Set SapModel = Nothing
      Set SapObject = Nothing
End Sub
```

APPENDIX B

CONDUCTING MULTI-SUPPORT EXCITATION USING SAP2000

In order to run MSE analysis in SAP2000, the excitations have to be defined as displacement time histories. This step can be done using SAP2000 by plotting the displacement response of the support after defining the excitation as acceleration time-history.

For the case of the Bayview bridge, four displacement time histories (Fig. B.1) were used. These displacement time histories were defined as functions using Define➔ Functions➔ TimeHistory.

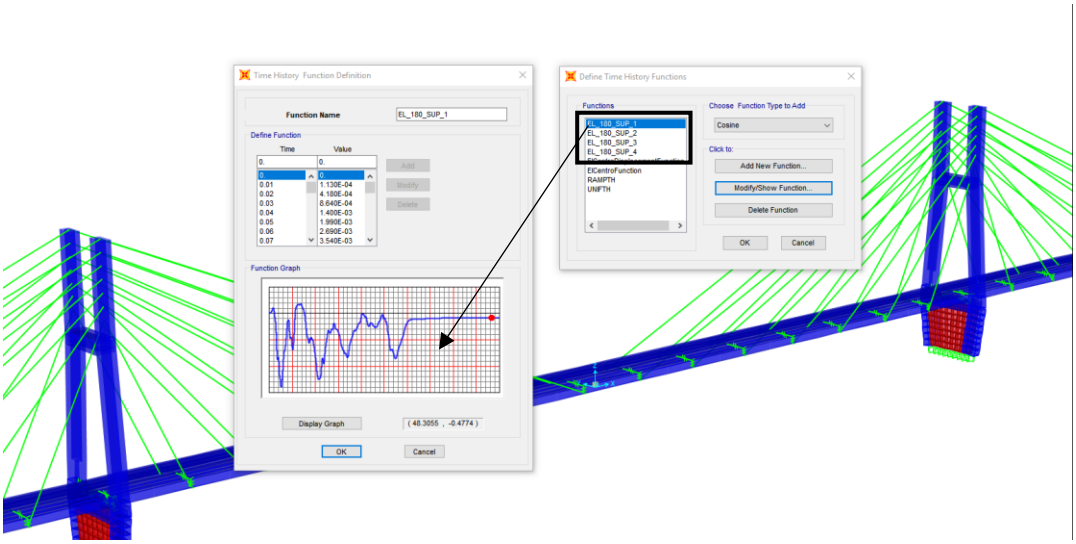

Figure B.1 Displacement time histories for MSE case.

Then, a load pattern for each direction and each support must be defined. In the case of the Bayview bridge and considering excitations in the longitudinal direction (*x-direction*), four load patterns were defined (Fig B.2) using Define➔ Load Patterns.

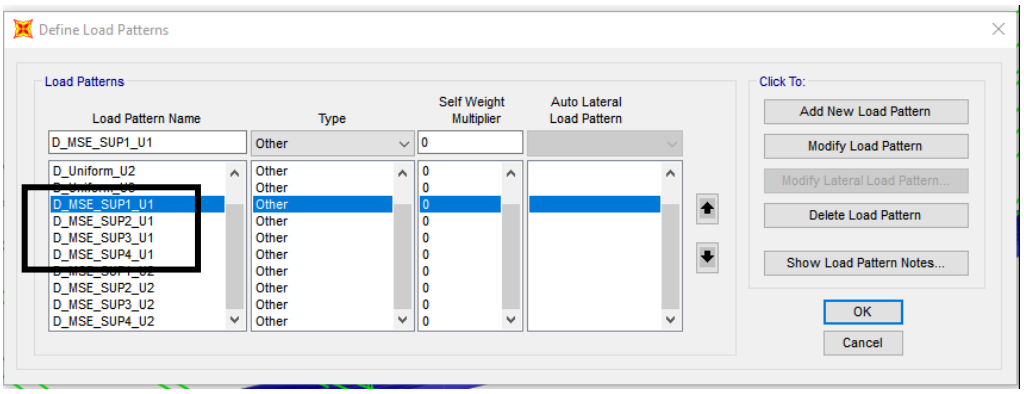

Figure B.2 Load patterns

The next step is to assign a unital displacement load to each support using the previously defined load patterns. For the Bayview bridge west tower support, a unital 1 inch displacement load under the pattern "D_MSE_SUP2_U1" was assigned (Fig B.3) using Assign➔Joint loads➔Displacements. However, similar process can be repeated for the other supports.

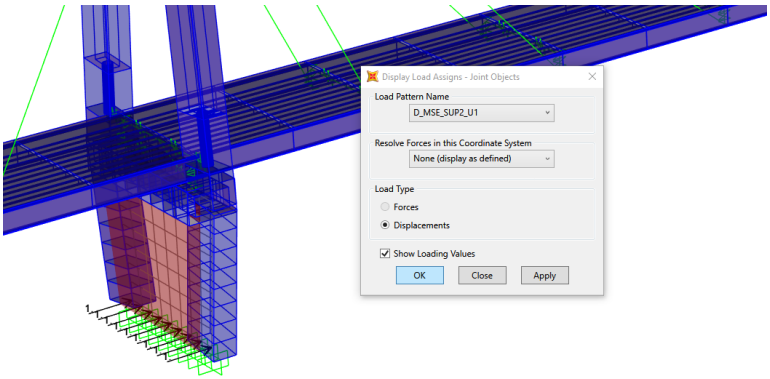

Figure B.3 West pylon unital load

The last step is to define a load case for the multi-support excitation which joints all the previously created load patterns (Fig. B.4) using Define➔ Load Cases. It is good to mention that for complicated modal shapes it is recommended to use Ritz vector modal analysis instead of Eigen vector analysis as it provides a faster approach to capture the responses for a fewer number of modes (Wilson 2004).

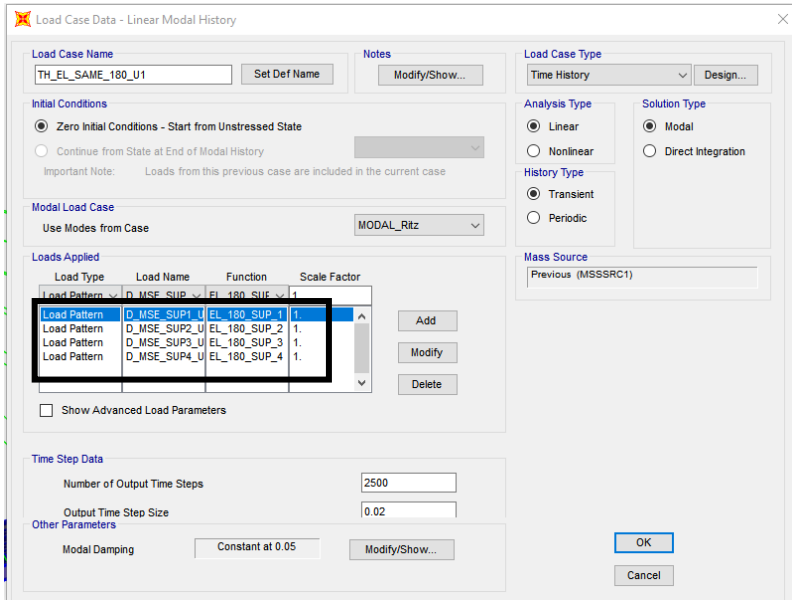

Figure B.4 MSE Load case definition

It is also critical to mention that the resulted responses are absolute not relative and to obtain the relative responses of a joint, a *generalized displacement* to be defined from the *Define* menu.